Organometallics **2003,** *22,* 2581−2593 2581

Alkynyl-Linked Poly(cobaltacarboranes). Directed Synthesis, Structures, and Electrochemistry of Linear Complexes and Benzene-Centered Pinwheels[1]

Haijun Yao, Michal Sabat, and Russell N. Grimes*

Department of Chemistry, University of Virginia, Charlottesville, Virginia 22901

Piero Zanello and Fabrizia Fabrizi de Biani

Dipartimento di Chimica dell'Università di Siena, Via Aldo Moro, 53100 Siena, Italy

Received February 27, 2003

A series of B(5)- and B(7)-alkynyl-substituted derivatives of CoC_2B_3, CoC_2B_4, and $Co_2C_2B_3$ cobaltacarboranes has been prepared and linked via metal-promoted cross-coupling reactions to generate several types of polynuclear molecular complexes, which were structurally characterized and studied via electrochemical techniques. The target compounds prepared include linear dicobalt species containing $BC{\equiv}CC{\equiv}CB$ linkages, e.g., $[Cp^*Co(2,3\text{-}Et_2C_2B_4H_3\text{-}7\text{-}C{\equiv}C)]_2$ (**8**) and $[Cp^*Co(2,3\text{-}Et_2C_2B_4H_3\text{-}5\text{-}C{\equiv}C)]_2$ (**17**), trigonally symmetrical 1,3,5-triethynylbenzene-anchored tricobalt and hexacobalt complexes, e.g., $\{Cp^*Co(2,3\text{-}Et_2C_2B_4H_3\text{-}5\text{-}C{\equiv}C)\}_3C_6H_3$ (**19**), $\{Cp^*Co(2,3\text{-}Et_2C_2B_4H_3\text{-}7\text{-}C{\equiv}C)\}_3C_6H_3$ (**22**), and 1,3,5-$[Cp^*{}_2Co_2(2,3\text{-}Et_2C_2B_3H_2\text{-}5\text{-}C{\equiv}C)]_3C_6H_3$ (**21**), and novel cobaltacarborane−Co_2C_2 mixed-cluster systems, e.g., $Cp^*Co(2,3\text{-}Et_2C_2B_4H_3)\text{-}7\text{-}C_2HCo_2(CO)_6$ (**5**) and $\{Cp^*Co[2,3\text{-}Et_2C_2B_4H_3\text{-}7\text{-}(C_2Co_2CO)_6]\}_3C_6H_3$ (**23**), a nonacobalt complex. The new compounds were obtained in all cases as air-stable crystalline solids and were characterized by multinuclear NMR and mass spectra, supplemented by X-ray diffraction data for **8**, **19**, and **21**. Electrochemical data on the alkynyl-linked compounds indicate that metal−metal communication in oxidized and reduced species occurs to a limited extent in most cases and to a considerable degree (Robin−Day class III) in the C_2B_3-bridged triple-decker systems.

Introduction

In the search for new molecule-based synthetic approaches to electronically tailorable nanostructured materials, conjugated polyynes are attracting increasing interest as conductive linkers between metal-containing electrophores.[2] At the same time, the special properties of small metallacarborane clusters make them attractive as building blocks for such systems as described below.[3] We are currently interested in combining these structural elements to create molecular complexes of specified design in which small metallacarborane units are connected by acetylenic chains (so-called "carbon wires") or other linkers and have developed general synthetic methods for achieving organosubsitution and linkage at boron vertexes.[4]

Using this approach, we have prepared and characterized a variety of iron- and cobalt-based systems featuring linear, branched, or macrocyclic geometries.[1,4] We have also examined the electrochemistry of selected poly(ferracarborane) systems in detail and interpreted these findings in light of DFT calculations.[5] Here we report the designed synthesis and properties of some new alkynyl-linked cobaltacarborane species having linear or branched architectures. In general, the small cobaltacarboranes have proved to be less reactive toward metal-catalyzed cross-coupling reactions than their ferracarborane analogues, an observation that we ascribe to the greater basicity of the Cp^*Co^{III} vs (arene)-Fe^{II} metal centers, which lowers the polarity of B−X bonds in the cobalt clusters relative to the iron compounds.

---

(1) Organotransition-Metal Metallacarboranes. 64. Part 63: Yao, H.; Sabat, M.; Grimes, R. N.; Fabrizi de Biani, F.; Zanello, P. *Angew. Chem., Int. Ed*. **2003**, *42*, 1002.

(2) Selected publications: (a) Werz, D. B.; Gleiter, R.; Rominger, F. *Organometallics* **2003**, *22*, 843. (b) Rigaut, S.; Perruchon, J.; Le Pichon, L.; Touchard, D.; Dixneuf, P. H. *J. Organomet. Chem*. **2003**, *670*, 37. (c) Bruce, M. I.; Costuas, K.; Halet, J.-F.; Hall, B. C.; Low, P. J.; Nicholson, B. K.; Skelton, B. W.; White, A. H. *J. Chem. Soc., Dalton Trans*. **2002**, 383. (d) Adams, R. D.; Qu, B.; Smith, M. D. *Inorg. Chem*. **2001**, *40*, 2932. (e) Yam, V. W.-W.; Zhang, L.; Tao, C.-H.; Wong, K. M.-C.; Cheung, K.-K. *J. Chem. Soc., Dalton Trans*. **2001**, 1111. (f) Paul, F.; Lapinte, C. *Coord. Chem. Rev*. **1998**, *178*−*180*, 431. (g) Siemsen, P.; Livingston, R. C.; Diederich, F. *Angew. Chem., Int. Ed*. **2000**, *39*, 2632. (h) Bunz, U. H. F. *Top. Curr. Chem*. **1999**, *201*, 131. (i) Bunz, U. H. F.; Roidl, G.; Altmann, M.; Enkelmann, V.; Shimizu, K. D. *J. Am. Chem. Soc*. **1999**, *121*, 10719. (j) Haley, M. M.; Bell, M. L.; English, J. J.; Johnson, C. A.; Weakley, T. J. R. *J. Am. Chem. Soc*. **1997**, *119*, 2956. (k) Guo, L.; Bradshaw, J. D., III; Tessier, C. A.; Youngs, W. J. *J. Chem. Soc., Chem. Commun*. **1994**, 243. (l) Dembinski, R.; Bartik, T.; Jaeger, M.; Gladysz, J. A., *J. Am. Chem. Soc*. **2000**, *122*, 810.

(3) Grimes, R. N. *Collect. Czech. Chem. Commun*. **2002**, *67*, 728.

(4) (a) Yao, H.; Sabat, M.; Grimes, R. N. *Organometallics* **2002**, *21*, 2833. (b) Russell, J. M.; Sabat, M.; Grimes, R. N. *Organometallics* **2002**, *21*, 4113. (c) Russell, J. M.; Sabat, M.; Grimes, R. N. *Organometallics* **2002**, *21*, 5613. (d) Malaba, D.; Sabat, M.; Grimes, R. N. *Eur. J. Inorg. Chem*. **2001**, 2557. (e) Bluhm, M.; Pritzkow, H.; Siebert, W.; Grimes, R. N. *Angew. Chem., Int. Ed*. **2000**, *39*, 4562; *Angew. Chem*. **2000**, *112*, 4736.

(5) Fabrizi de Biani, F.; Fontani, M.; Ruiz, E.; Zanello, P.; Russell, J. M.; Grimes, R. N. *Organometallics* **2002**, *21*, 4129.

10.1021/om0301379 CCC: $25.00
Publication on Web 05/17/2003

Results and Discussion

Synthetic Strategies. Several advantages are afforded by the seven-vertex MC_2B_4 clusters as building-block units.[3,6]

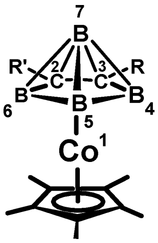

(a) Monosubstitution at boron is restricted to just three electronically distinguishable locations (B(4,6), B(5), and B(7)), which greatly simplifies the synthesis and isolation of specific isomers compared to larger (e.g., icosahedral) cluster systems. By employing appropriate synthetic methods, substituents may be introduced either on the mirror plane at equatorial (B(5)) or apical (B(7)) vertexes to give nonchiral products or at B(4) or B(6) to generate chiral derivatives; chirality can also be introduced via use of inequivalent groups on the cage carbons ($R \neq R'$).[7]

(b) Substitution at boron can be controlled by adjustment of reaction conditions to generate specific B-functional target compounds in good yield.

(c) Removal of the apex boron (decapitation) affords *nido*-MC_2B_3 complexes that further extend the range of synthetic possibilities and reactivities.

(d) In B(5,7) difunctional MC_2B_4 complexes, the equatorial and apical substituents are orthogonal, allowing the construction of oligomers and extended systems having square or rectangular patterns.[1] The 7-vertex metallacarboranes thus complement, as structural modules, the icosahedral boron-based C_2B_{10} carboranes and other 12-vertex clusters whose more spherical cage geometry lends itself to quite different molecular architectures.[8]

In this paper we describe the introduction of ethynyl groups at equatorial (B(5)) and apical (B(7)) vertexes, selected examples of reactivity of the C≡C substituents, their linkage to create diethynyl-linked dimers for use in building larger systems, and their incorporation into benzene-centered pinwheel-type polynuclear complexes.

Alkynyl Substitution and Linkage at B(7). As was shown earlier[4b] in (arene)FeC_2B_4 cluster chemistry, the introduction of alkynyl substituents at the apex boron can be accomplished either by attack of alkynylzinc reagents at B(7)−halogen atoms or by insertion of a B−alkynyl moiety into an open-cage (nido) MC_2B_3 complex anion (Scheme 1, top). In this work, the most efficient synthesis of the B(7)−ethynyl(trimethylsilyl) derivative **2** was achieved via treatment of the B(7)−iodo complex **3b** to afford **2** in nearly quantitative yield. Desilylation of **2** with fluoride ion gave the very useful B(7)−ethynyl complex **4**, which serves as a precursor to a variety of apically substituted cobaltacarborane derivatives, as shown. Thus, reaction of **4** with dicobalt octacarbonyl in pentane at room temperature afforded the mixed-cluster species $Cp^*Co(2,3\text{-}Et_2C_2B_4H_3)\text{-}7\text{-}C_2\text{-}HCo_2(CO)_6$ (**5**) in 88% yield. This compound, which we believe to be the first reported metallacarborane−C_2M_2 system, was isolated as a dark red air-stable solid and characterized via multinuclear NMR, UV−visible, and IR spectroscopy and elemental analysis. An example of multiple conversion of alkynyl groups in the same molecule to M_2C_2 clusters is reported below.

In a multistep sequence (Scheme 1), the ethynyl group in **4** was deprotonated with *tert*-butyllithium and coupled to $Me_3SiC{\equiv}C$, the product was iodinated at B(5) to generate **6**, and the TMS group was removed to give the B(7)−diethynyl B(5)−iodo derivative **7**.

Direct alkynyl coupling of **4** via reaction with CuI and pyridine yielded the dimer **8**, and palladium-promoted cross-coupling with *p*-iodobenzoic acid gave, on acidification with HCl, the B(7)−alkynylbenzoic acid complex **9**. Characterization of these species, as with all new compounds reported herein, is based on spectroscopy and elemental analysis, supported in three cases by X-ray crystallography.

The expected B(7),B(7′)−diethynyl-linked molecular structure of **8** was confirmed by X-ray diffraction (Figure 1 and Tables 1 and 2), and the molecule was found to adopt a centrosymmetric conformation in the crystal. The diethynyl chain is linear, with C(4)−C(5)−C(5*) and C(5)−C(4)−B(7) angles of 179.2 and 176.9°, respectively; the CoC_2B_4 cluster bond distances and angles are normal, and the Cp* and carborane rings bound to cobalt are nearly parallel with a dihedral angle of 4.8°.

Alkynyl Substitution and Linkage at B(5). Scheme 2 shows the conversions of B(5)−iodo *closo*- and *nido*-cobaltacarboranes (**10** and **13**, respectively) to the corresponding B(5)−ethynyl(trimethylsilyl) derivatives **11** (prepared earlier in lower yield[4c] from the Co(II) radical anion $\mathbf{10}^-$) and **14**, followed by their desilylation to give **12** and **15**, respectively. The open-cage complex **14** was bridge-deprotonated with butyllithium and reacted with $(Cp^*CoCl)_2$ to afford the B(5)−ethynyl(trimethylsilyl)ated triple-decker sandwich **16**, which we had envisioned as a potentially useful reagent for introducing $(Cp^*Co)_2(Et_2C_2B_3H_2)\text{-}5\text{-}C{\equiv}C{-}$ alkynyl triple-decker substituents. However, this complex has proved surprisingly unreactive and resists desilylation, even with strong reagents such as MeOH/NaOH and CH_3COOH/Bu_4NF.

Dimerization of **12** by treatment with palladium and copper(I) gave the desired B(5),B(5′)−diethynyl-linked product **17** in 66% isolated yield. This compound was doubly deboronated (decapped) with TMEDA to afford the *nido*-cobaltacarborane dimer **18**; the latter compound was also obtained from **15** by reaction with

---

[6] Grimes, R. N. In *Contemporary Boron Chemistry*; Davidson, M., Hughes, A. K., Marder, T. B., Wade, K., Eds.; Royal Society of Chemistry: London, 2000; p 283.

[7] (a) Benvenuto, M. A.; Grimes, R. N. *Inorg. Chem.* **1992**, *31*, 3897. (b) Benvenuto, M. A.; Sabat, M.; Grimes, R. N. *Inorg. Chem.* **1992**, *31*, 3904.

[8] For recent overviews see: (a) Colquhoun, H. M.; Lewis, D. F.; Herbertson, P. L.; Wade, K.; Baxter, I.; Williams, D. J. In *Contemporary Boron Chemistry*; Davidson, M., Hughes, A. K., Marder, T. B., Wade, K., Eds.; Royal Society of Chemistry: London, 2000; p 59. (b) Grimes, R. N. In *Organic Synthesis Highlights III*; Mulzer, J., Waldmann, H., Eds.; Wiley-VCH: New York, 1998; p 406. Leading references: (c) Zheng, Z.; Knobler, C. B.; Mortimer, M. D.; Kong, G.; Hawthorne, M. F. *Inorg. Chem.* **1996**, *35*, 1235. (d) Jiang, W.; Knobler, C. B.; Mortimer, M. D.; Hawthorne, M. F. *Angew. Chem., Int. Ed. Engl.* **1995**, *34*, 1332. (e) Jiang, W.; Knobler, C. B.; Hawthorne, M. F. *Inorg. Chem.* **1996**, *35*, 3056. (f) Schoeberl, U.; Magnera, T. F.; Harrison, R. M.; Fleischer, F.; Pflug, J. L.; Schwab, P. F. H.; Meng, X.; Lipiak, D.; Noll, B. C.; Allured, V. S.; Rudalevige, T.; Lee, S.; Michl, J., *J. Am. Chem. Soc.* **1997**, *119*, 3907.

Scheme 1. B(7)−Alkynyl Substitution and Linkage[a]

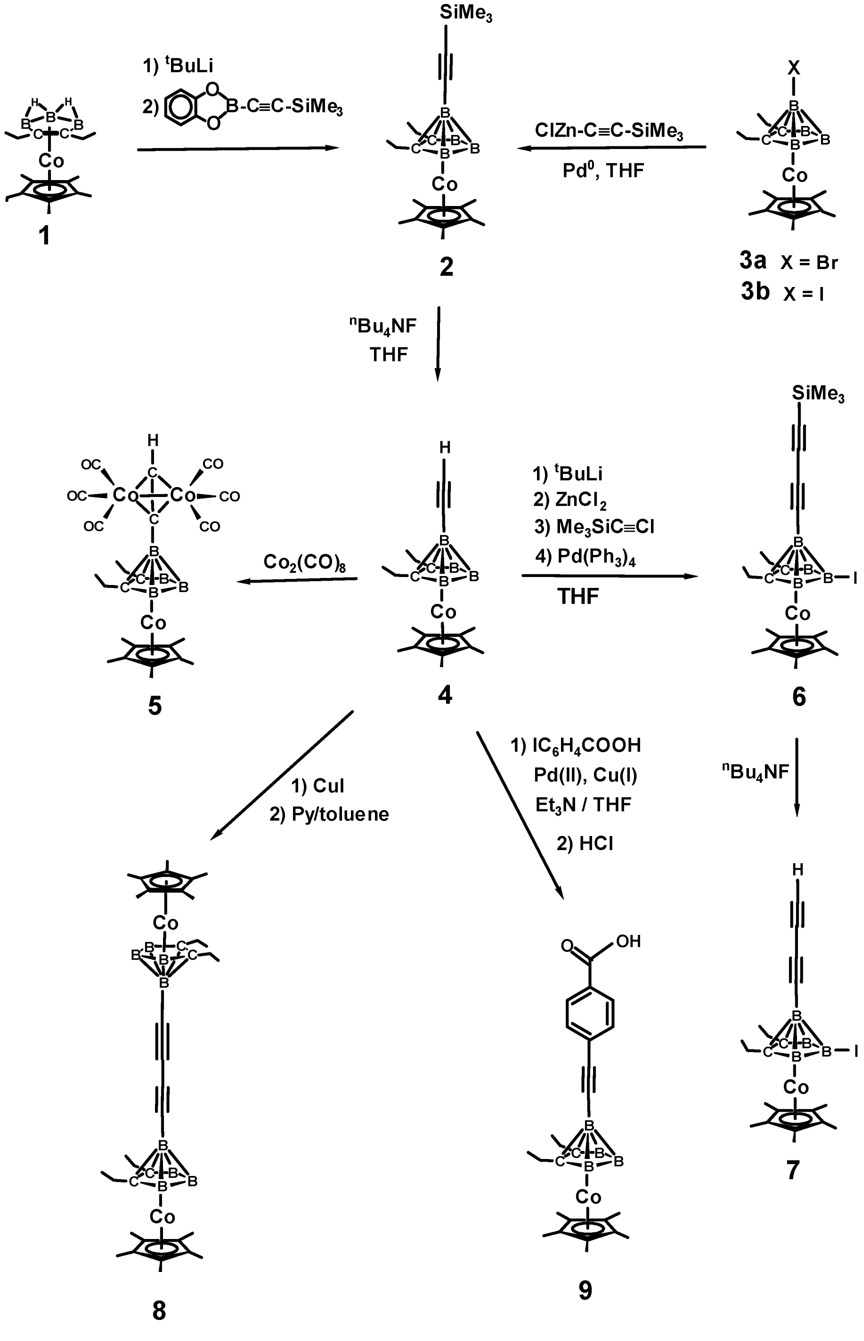

[a] B = B, BH.

chloroacetone and triethylamine. As in the case of their B(7)−alkynyl isomers, the equatorially functionalized B(5)−alkynyl complexes are designed as structural modules for the assembly of larger systems of specific design, as will be illustrated here.

Construction of Benzene-Centered Pinwheel Complexes. The concept of anchoring multiple metallacarborane units to a central hydrocarbon ring reverses the paradigm of using boron clusters as scaffolds for hydrocarbon appendages that has been effectively employed by several groups.[8] Benzene offers several advantages in this role, including stability, high symmetry, π-aromaticity (allowing it to function as an electron conduit), and ready availability of 1,3,5-trifunctional derivatives. Recent papers from one of our laboratories[4b,e] have described the synthesis of several ferracarborane−benzenoid metallacarborane pinwheels, and a preliminary communication[4a] reported a benzene-centered tris(triple-decker) cobaltacarborane complex. Here we present a full report including several new cobalt-based systems of this class.

Reaction of 1,3,5-triiodobenzene with the B(5)−ethynyl *closo*-cobaltacarborane **12** in THF generated the tris(cobaltacarboranyl)benzene complex **19**, a yellow solid, in 60% isolated yield, as shown in Scheme 3. The trigonally symmetric structure (idealized C_{3h} point group in the conformation represented in Scheme 3) is supported by multinuclear NMR spectra, which are consistent with three equivalent Cp*Co^{III}(Et$_2$C$_2$B$_4$H$_3$)-5-C≡C− units, and has been confirmed by X-ray diffraction analysis (Figure 2 and Tables 1 and 3). The complex crystallizes in the rhombohedral space group

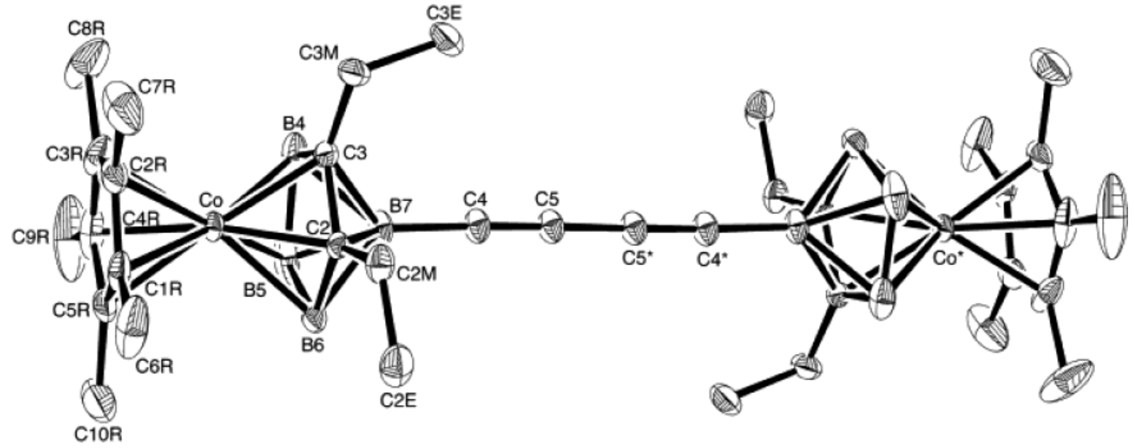

Figure 1. Ortep diagram of $[Cp^*Co(2,3\text{-}Et_2C_2B_4H_3\text{-}7\text{-}C{\equiv}C)]_2$ (**8**) (hydrogens omitted).

Table 1. Experimental X-ray Diffraction Parameters and Crystal Data

	8	19
empirical formula	$C_{36}H_{56}B_8Co_2$	$C_{60}H_{87}B_{12}Co_3$
fw	693.15	1114.81
cryst dimens (mm)	0.28 × 0.12 × 0.12	0.25 × 0.14 × 0.12
space group	$R\bar{3}$ (No. 148, hexagonal setting)	$P2_1/c$ (No. 14)
a, Å	35.425(1)	8.6443(6)
b, Å	35.425(1)	23.318(2)
c, Å	8.3845(4)	30.425(2)
α, deg	90	90
β, deg	90	92.748(2)
γ, deg	120	90
V, Å^3	9112.3(6)	6125.7(8)
Z	9	4
D(calcd), g cm^{-3}	1.137	1.209
μ(Mo Kα), mm^{-1}	0.842	0.839
temp, K	153(2)	153(2)
$2\theta_{max}$, deg	65	65
transmissn factors	0.59−0.80	0.73−0.80
no. of rflns collected	42 276	84 352
no. of obsd rflns ($I > 2\theta(I)$)	7283	22 126
no. of params refined	227	733
R	0.0516	0.0598
R_w	0.1651	0.1296
goodness of fit	1.471	0.954
largest peak in final diff map, e/Å^3	1.048	0.926

Table 2. Selected Distances (Å) and Angles (deg) for 8[a]

Co−C(2)	2.0264(16)	C(3)−B(7)	1.777(3)
Co−C(3)	2.0275(17)	C(2E)−C(2M)	1.523(4)
Co−B(4)	2.099(2)	C(3E)−C(3M)	1.534(3)
Co−B(5)	2.114(2)	C(2)−C(2M)	1.508(3)
Co−B(6)	2.081(2)	C(3)−C(3M)	1.517(3)
Co−C(1R)	2.0502(18)	C(4)−C(5)	1.208(2)
Co−C(2R)	2.0671(19)	C(4)−B(7)	1.530(3)
Co−C(3R)	2.036(2)	C(5)−C(5*)	1.373(4)
Co−C(4R)	2.014(2)	B(4)−B(5)	1.692(5)
Co−C(5R)	2.015(2)	B(4)−B(7)	1.793(4)
C(2)−C(3)	1.468(2)	B(5)−B(6)	1.681(4)
C(2)−B(6)	1.562(3)	B(5)−B(7)	1.750(3)
C(2)−B(7)	1.765(3)	B(6)−B(7)	1.783(3)
C(3)−B(4)	1.554(3)		

C(3)−C(2)−B(6)	112.58(17)	C(4)−B(7)−C(2)	123.30(17)
C(2)−C(3)−B(4)	112.87(18)	C(4)−B(7)−C(3)	124.70(17)
C(3)−B(4)−B(5)	104.85(19)	C(4)−B(7)−B(4)	132.30(19)
C(2)−B(6)−B(5)	104.94(19)	C(4)−B(7)−B(5)	137.78(16)
B(6)−B(5)−B(4)	104.75(17)	C(5)−C(4)−B(7)	176.9(2)
C(4)−B(7)−B(6)	130.18(19)	C(4)−C(5)−C(5*)	179.2(3)

[a] Symmetry transformations used to generate equivalent atoms: (#1) $-x + {}^1/_3, -y - {}^1/_3, -z + {}^5/_3$.

$R\bar{3}$. Bond distances and angles are normal, and the parameters of the cobaltacarborane cage are within the usual range for *closo*-1,2,3-CoC_2B_4 pentagonal-bipyramidal clusters. The Cp* and C_2B_3 ring planes are not quite parallel, with a dihedral angle of 4.8°, and are tilted with respect to the central benzene ring (see Figure 2), an observation we attribute to crystal-packing forces that favor a relatively flattened molecular conformation.

Complex **19** is isostructural and isoelectronic with the tris(ferracarboranyl)benzene compound 1,3,5-$[(\eta^6\text{-}C_6H_6)\text{-}Fe^{II}(Et_2C_2B_4H_3)\text{-}5\text{-}C{\equiv}C]_3C_6H_3$ (**19-Fe),** which was recently prepared in our laboratory by palladium-promoted coupling of $(\eta^6\text{-}C_6H_6)Fe(Et_2C_2B_4H_3)\text{-}5\text{-}C{\equiv}CH$ to 1,3,5-triiodobenzene.[4b]

Reaction of the *nido*-cobaltacarborane **15**, obtained by decapping of **12** in aqueous TMEDA, with 1,3,5-$C_6H_3I_3$ afforded the yellow-orange pinwheel complex **20** (Scheme 3), which was isolated via column chromatography in 87% yield and characterized spectroscopically. Triple face-deprotonation of this complex with NaH gave the trianion $\mathbf{20}^{3-}$**,** which reacted with $(Cp^*CoCl)_2$ to afford the dark red air-stable tris(triple-decker sandwich) complex **21** in 69% yield. From NMR data on **21** it is clear that the six Cp* ligands, and hence the six cobalt centers, are electronically equivalent, consistent with the structure depicted in Scheme 3; this geometry has been confirmed crystallographically (Figure 3), as reported in a recent communication[4a] (details of the structure determination are available as Supporting Information for ref 4a). As in **19**, the C_2B_3 rings in the solid state are significantly rotated away from coplanarity with the benzene ring and, indeed, are nearly perpendicular to it, but free rotation around the ethynyl axes is assumed in solution.

The apically substituted complex $Cp^*Co^{III}(Et_2C_2B_4H_3)\text{-}7\text{-}C{\equiv}CH$ (**4**) was treated with *n*-butyllithium and zinc chloride and finally with 1,3,5-$C_6H_3I_3$ to generate the benzene-centered product 1,3,5-$[Cp^*Co^{III}(Et_2C_2B_4H_3)\text{-}7\text{-}C{\equiv}C]_3C_6H_3$ (**22**), isolated as an orange-yellow solid in 81% yield. In an alternative approach, the reaction of a mixture of **4**, $Pd(PPh_3)_2Cl_2$, CuI, $C_6H_3I_3$, and Et_3N in THF over 2 days gave **22** in 66% yield. The structural characterization of **22** is based on multinuclear NMR and other spectroscopic data, which showed trigonal symmetry having equivalent cobaltacarborane cluster

Scheme 2. B(5)−Alkynyl Substitution and Linkage[a]

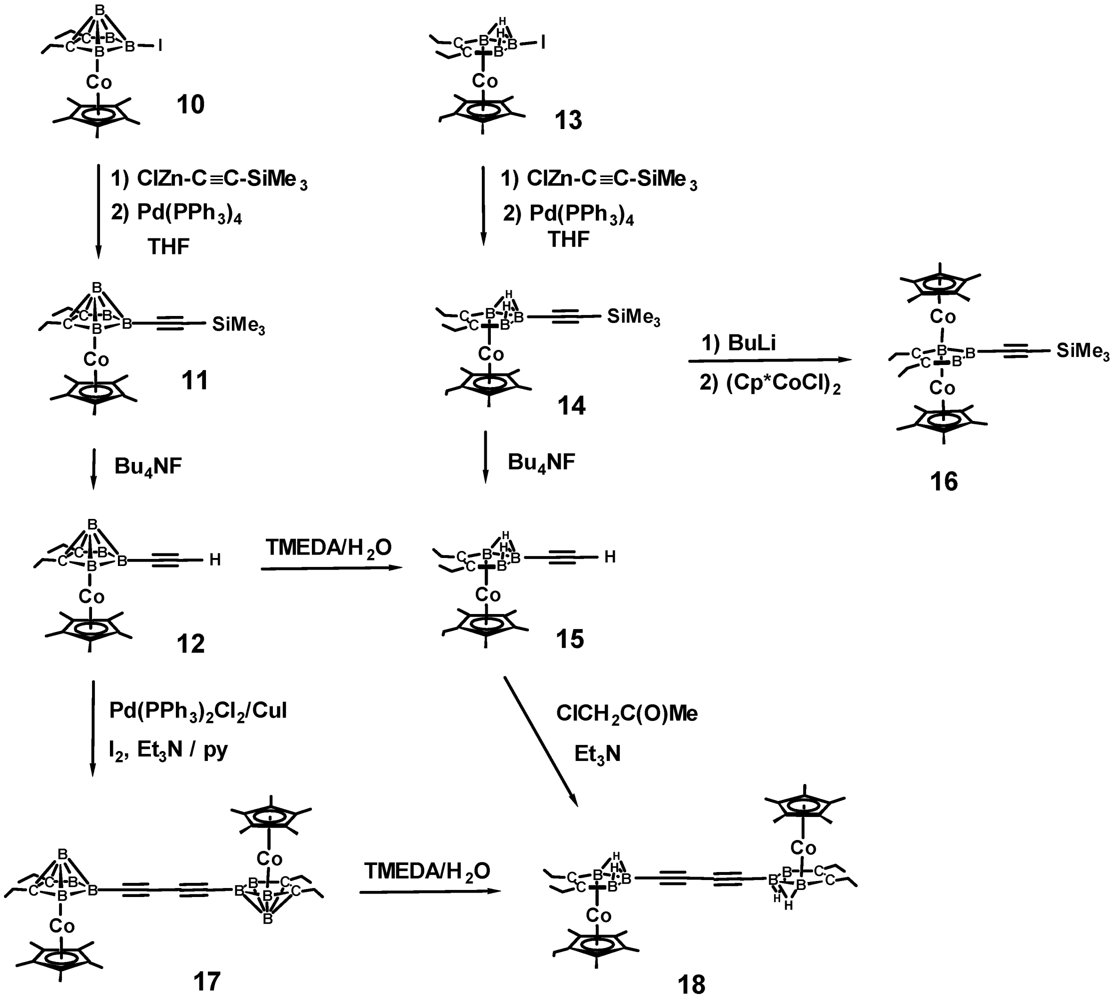

[a] B = B, BH.

units, as in the case of **19**, discussed above. Although **19** and its isomer **22** are spectroscopically similar, any possible ambiguity concerning their identities is eliminated by the crystallographically established structure on **19**; hence, the apically bound geometry for **22** shown in Scheme 3, which is the only other structure consistent with the NMR data, is clear.

Reaction of **22** with dicobalt octacarbonyl at room temperature in dichloromethane afforded in 55% yield the red-brown nonacobalt complex **23**. Although apparently high-quality crystals were obtained, repeated attempts to obtain X-ray data on this compound have been unsuccessful, owing to loss of solvent from the crystals. However, the ^{11}B, ^{1}H, and ^{13}C NMR, UV−visible, and IR spectroscopic data combined with elemental analysis are consistent with the structure depicted in Scheme 3. The close similarity of these spectra to those of **22** strongly supports the proposed trigonally symmetric structure.

Electrochemistry. Several of the compounds described above were selected for detailed examination, and the potentials for the observed redox changes are compiled in Table 4.

Figure 4 compares the cyclic voltammetric behavior of the binuclear complex **17** (bottom) with that of the mononuclear precursor Cp*Co^{III}(Et$_2$C$_2$B$_4$H$_4$) (top), in CH$_2$Cl$_2$ solution. Cp*Co^{III}(Et$_2$C$_2$B$_4$H$_4$) undergoes a reversible one-electron oxidation,[9] ascribed to the redox change Co^{III}/Co^{IV}. The corresponding process for the dimer **17** seems to occur as a single two-electron step complicated by following chemical reactions, although the rapid increase in the solvent discharge may mask the second process. In this case, however, two very close one-electron reductions appear, which imply a small degree of electronic communication between the two cobalt centers. Given that the observation of separate redox processes in molecules containing multiple redox-active centers allows easy determination of the comproportionation constant K_{com},[10] one may attempt to correlate this value with the nature of the electrogenerated mixed-valent species. In fact, it is commonly accepted[11] that the value of the comproportionation constant is linked to the extent of charge delocalization in mixed-valent species according to the Robin−Day classification.[12] However, it must be kept in mind that the value of K_{com} is affected by a number of factors, including electrostatic repulsion, statistical effects, inductive effects, and magnetic exchanges.[13] On this basis, the 0.05 V separation between the redox potentials of the two

---

(9) Stephan, M.; Hauss, J.; Zenneck, U.; Siebert, W., Grimes, R. N. *Inorg. Chem.* **1994**, *33*, 4211.

(10) Richardson, D. E.; Taube, H. *Inorg. Chem.* **1981**, *20*, 1278.

(11) Bott, A. W. *Curr. Sep.* **1997**, *16*, 61 and references therein.

(12) Robin, M. B.; Day, P. *Adv. Inorg. Chem. Radiochem.* **1967**, *10*, 247.

Scheme 3. Construction of Pinwheel Complexes[a]

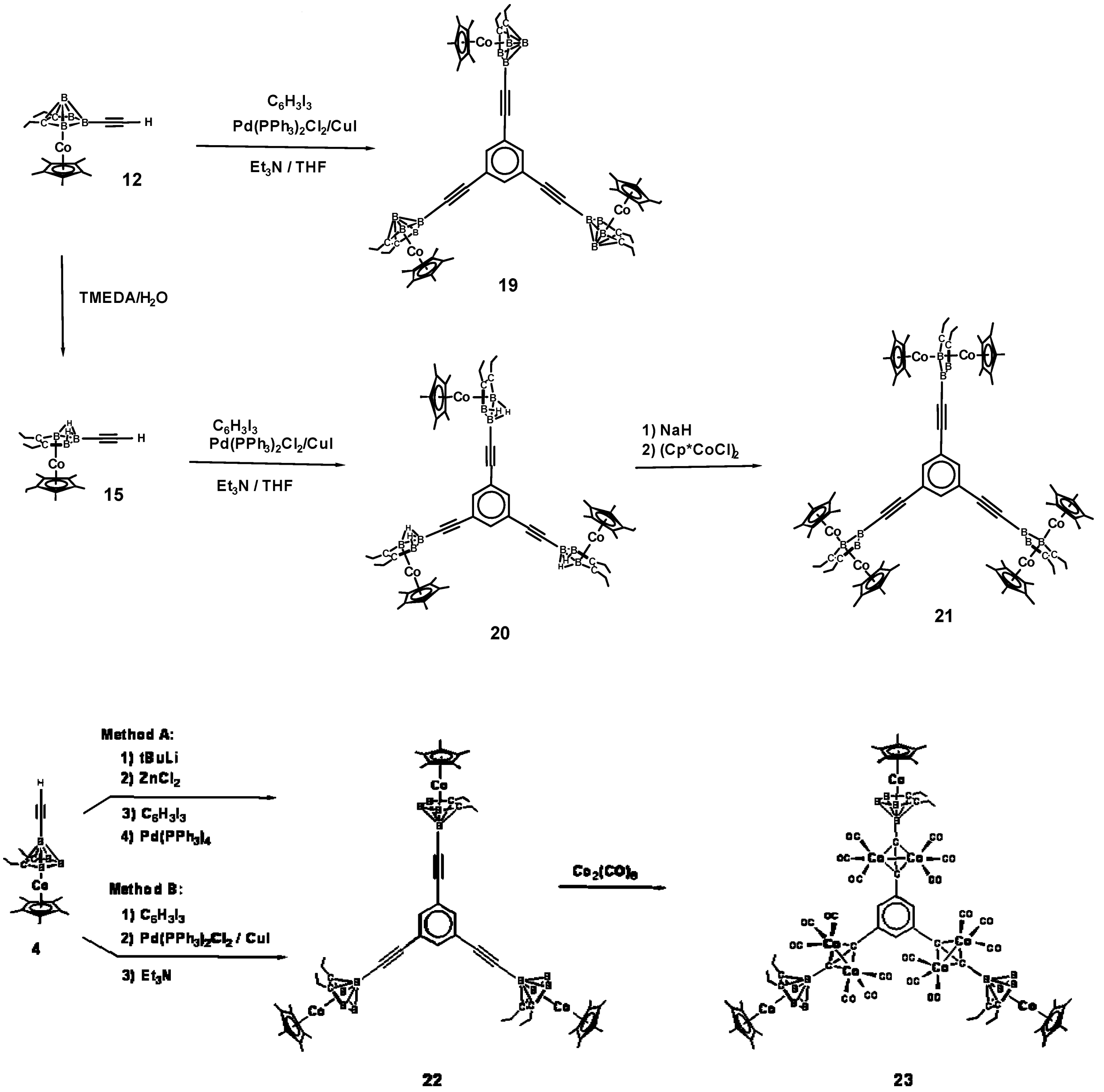

[a] B = B, BH.

electron additions suggests that the mixed-valence species **17**$^-$ could be tentatively assigned to the localized Robin–Day class I ($K_{com} \approx 10$). Similar results were obtained using tetrahydrofuran as solvent.

The B(7)–B(7′)-connected dimer **8** exhibits electrochemical behavior that qualitatively resembles that of its B(5)–B-(5′) isomer **17**, but the separation between the two cathodic processes is larger ($K_{com} \approx 10^2$), suggesting that Co–Co communication is greater in **8** than in **17**.

Turning to the trinuclear complexes, Figure 5 illustrates the redox behavior of complex **22** under experimental conditions (see the figure caption) that were chosen to highlight its main features. In particular, the anodic pathway was followed using the weakly coordinating $[NBu_4][B(C_6F_5)_4]$ supporting electrolyte.[14]

As seen, **22** undergoes three sequential reductions and three sequential oxidations, each having features of chemical reversibility on the cyclic voltammetric time scale. For the sake of simplicity, and taking into account the number of cobaltacarborane subunits, we assume that each step involves a one-electron process. The results are consistent with the presence of electronic communication to a small extent between the three cobaltacarborane subunits. This finding again demonstrates that the intramolecular interaction in multicentered molecules depends on the nature of both the metal-containing units and the interposed spacers. It was shown earlier by Zanello and co-workers[15] that tris(ferrocenylethynyl)benzene exhibits only a single three-electron, ferrocene-centered oxidation; in tris(cyclopen-

---

(13) (a) Palaniappan, V.; Singru, R. M.; Agarwala, U. C. *Inorg. Chem.* **1988**, *27*, 181. (b) Astruc, D. *Electron Transfer and Radical Processes in Transition-Metal Chemistry*; Wiley-VCH: New York, 1995. (c) Brunschwig, B. S.; Sutin, N. *Coord. Chem. Rev.* **1999**, *187*, 233. (d) Demadis, K. D.; Hartshorn, C. M.; Meyer, T. J. *Chem. Rev.* **2001**, *101*, 2655. (e) Barriere, F.; Camire, N.; Geiger, N. E.; Mueller-Westerhoff, T. U.; Sanders, R. *J. Am. Chem. Soc.* **2002**, *124*, 7262.

(14) LeSuer, R. J.; Geiger, W. *Angew. Chem., Int. Ed.* **2000**, *39*, 248.

(15) Fink, A. H.; Long, N. J.; Martin, A. J.; Opromolla, G.; White, A. J. P.; Williams, D. J.; Zanello, P. *Organometallics* **1997**, *16*, 2646.

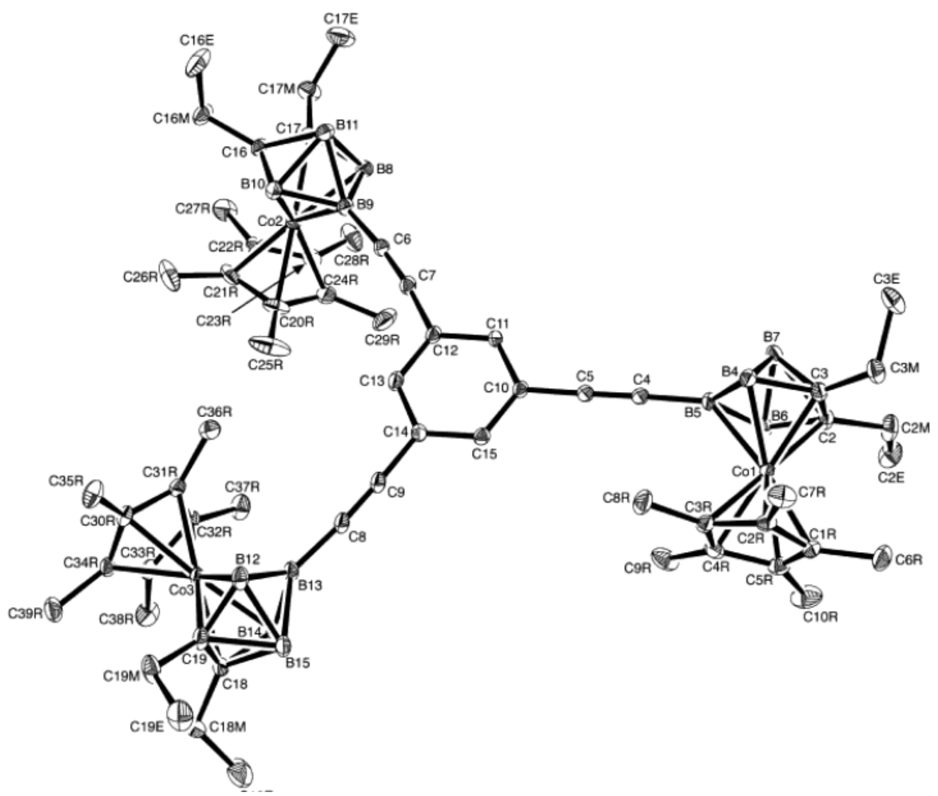

Figure 2. Ortep diagram of $\{Cp^*Co(2,3\text{-}Et_2C_2B_4H_3\text{-}5\text{-}C{\equiv}C)\}_3C_6H_3$ (**19**) (hydrogens omitted).

tadienylruthenium diphosphine ethynyl)benzene[16] three slightly separated one-electron oxidations occur, as observed by Weyland et al. in the tris(cyclopentadienyliron diphosphine ethynyl)benzene.[17]

It is also noteworthy that, in both the cathodic and the anodic scans, the separation between the first and the second step is 0.2 V, while that between the second and the third steps is only 0.1 V. Since such behavior is in contrast to that expected on the basis of Coulombic effects, it can be interpreted as arising from the attenuation of the electronic interaction on passing from the monocharged $[\mathbf{22}]^+$ or $[\mathbf{22}]^-$ species to the corresponding bicharged $[\mathbf{22}]^{2+}$ or $[\mathbf{22}]^{2-}$species.

In contrast to **22**, for complex **19** we were able to resolve the three-electron oxidation into only two separate steps, while the three-electron reduction remained completely unresolved. These data suggest that any mixed-valent species $[\mathbf{19}]^{n+/n-}$ ($n = 1, 2$) will belong to localized Robin–Day class I.

Let us now discuss the triple-decker complex **16** and its trimeric counterpart **21**, whose voltammetric patterns are shown in Figure 6.

Complex **16** undergoes two separate oxidations and two separate reductions. Controlled-potential coulometry corresponding to the first anodic process ($E_w = +0.4$ V) shows the consumption of one electron per molecule. Cyclic voltammetric tests on the resulting solution indicate that the electrogenerated cation $\mathbf{16}^+$ undergoes minor decomposition. Both the second one-electron addition and the second one-electron removal appear to be chemically irreversible. Accordingly, the mixed-valent congeners $\mathbf{16}^+$ and $\mathbf{16}^-$ can be assigned to the completely delocalized Robin-Day class III ($K_{com} = 6.5 \times 10^{21}$ and 5.4×10^{16}, respectively). In this light, the redox behavior of **16** is quite reminiscent of that of the related complexes $(p\text{-}MeC_6H_4CHMe_2)_2Ru_2(Et_2C_2B_3H_3)$ and $CpCo(Et_2C_2B_3H_3)Ru(p\text{-}MeC_6H_4CHMe_2)$,[18] the cations of which are also classified as fully delocalized mixed-valent species. These results underline the ability of bridging $(R_2C_2B_3H_3)^{4-}$ ligands to allow very strong electronic interactions between two η^5-coordinated metallic centers in multidecker sandwich systems, as originally shown by Geiger.[19]

The redox behavior of the related trimer **21** resembles that of **16**, in that it undergoes oxidation and reduction processes at similar potential values. Nevertheless, as shown in Figure 6, the use of $[NBu_4][B(C_6F_5)_4]$ as electrolyte allowed us to resolve the first oxidation in three very close sequential processes. In support of this observation, controlled-potential coulometry ($E_w = +0.4$ V) showed the involvement of three electrons per molecule. Upon oxidation the original orange solution turned brown, and, as was also the case for $\mathbf{16}^+$, cyclic voltammetry indicated that the electrogenerated trication $\mathbf{21}^{3+}$ undergoes some minor decomposition.

Finally, complex **20** exhibited only a quasi-reversible electron reduction accompanied by chemical complications. The relative square-wave voltammogram can be simulated by three subsequent processes. Actually, the solution resulting from exhaustive cathodic reduction ($E_w = -1.2$ V) gave a voltammetric pattern quite close to that of the monomeric precursor $Cp^*Co^{III}(Et_2C_2B_3H_5)$, which in contrast to $Cp^*Co^{III}(Et_2C_2B_4H_4)$ undergoes an irreversible oxidation process.

---

[16] Long, N. J.; Martin, A. J.; Fabrizi de Biani, F.; Zanello, P. *J. Chem. Soc., Dalton Trans.* **1998**, 2017.

[17] Weyland, T.; Lapinte, C.; Frapper, G.; Calhorda, M. J.; Halet, J.-F.; Toupet, L. *Organometallics* **1997**, *16*, 2024.

[18] Merkert, J. W.; Davis, J. H.; Geiger, W. E.; Grimes, R. N. *J. Am. Chem. Soc.* **1992**, *114*, 9846.

[19] Brennan, D. E.; Geiger, W. E., Jr. *J. Am. Chem. Soc.* **1979**, *101*, 3399.

Table 3. Selected Distances (Å) and Angles (deg) for 19

Co(1)−C(3)	2.034(3)	C(12)−C(13)	1.392(4)
Co(1)−C(2)	2.042(3)	C(13)−C(14)	1.395(4)
Co(1)−B(4)	2.091(3)	C(14)−C(15)	1.395(3)
Co(1)−B(6)	2.095(3)	C(16)−C(17)	1.473(4)
Co(1)−B(5)	2.107(3)	C(16)−C(16M)	1.513(4)
Co(2)−C(17)	2.030(3)	C(16)−B(10)	1.524(5)
Co(2)−C(16)	2.033(3)	C(16)−B(11)	1.770(4)
Co(2)−B(10)	2.080(4)	C(16E)−C(16M)	1.511(4)
Co(2)−B(8)	2.091(3)	C(17)−C(17M)	1.514(4)
Co(2)−B(9)	2.115(3)	C(17)−B(8)	1.558(4)
Co(3)−C(18)	2.030(3)	C(17)−B(11)	1.761(4)
Co(3)−C(19)	2.021(3)	C(17E)−C(17M)	1.506(4)
Co(3)−B(14)	2.083(3)	C(18)−C(19)	1.479(4)
Co(3)−B(12)	2.091(3)	C(18)−C(18M)	1.510(4)
Co(3)−B(13)	2.123(3)	C(18)−B(14)	1.544(4)
C(2)−C(3)	1.477(4)	C(18)−B(15)	1.759(4)
C(2)−C(2M)	1.510(4)	C(18E)−C(18M)	1.459(5)
C(2)−B(6)	1.552(4)	C(19)−C(19M)	1.505(4)
C(2)−B(7)	1.777(4)	C(19)−B(12)	1.547(4)
C(2E)−C(2M)	1.502(4)	C(19)−B(15)	1.770(4)
C(3)−C(3M)	1.514(4)	C(19E)−C(19M)	1.517(4)
C(3)−B(4)	1.563(4)	B(4)−B(5)	1.680(4)
C(3)−B(7)	1.772(4)	B(4)−B(7)	1.790(4)
C(3E)−C(3M)	1.527(4)	B(5)−B(6)	1.680(4)
C(4)−C(5)	1.205(3)	B(5)−B(7)	1.744(4)
C(4)−B(5)	1.522(4)	B(6)−B(7)	1.789(5)
C(5)−C(10)	1.436(3)	B(8)−B(9)	1.672(5)
C(6)−C(7)	1.206(4)	B(8)−B(11)	1.783(5)
C(6)−B(9)	1.516(4)	B(9)−B(10)	1.684(4)
C(7)−C(12)	1.435(4)	B(9)−B(11)	1.751(4)
C(8)−C(9)	1.200(4)	B(10)−B(11)	1.775(5)
C(8)−B(13)	1.528(4)	B(12)−B(13)	1.679(4)
C(9)−C(14)	1.439(4)	B(12)−B(15)	1.786(5)
C(10)−C(11)	1.392(3)	B(13)−B(14)	1.682(5)
C(10)−C(15)	1.402(3)	B(13)−B(15)	1.747(4)
C(11)−C(12)	1.396(3)	B(14)−B(15)	1.790(5)

C(3)−C(2)−B(6)	112.4(2)	C(17)−C(16)−B(10)	112.2(2)
C(2)−C(3)−B(4)	112.7(2)	C(16)−C(17)−B(8)	112.6(2)
C(5)−C(4)−B(5)	176.0(3)	C(19)−C(18)−B(14)	112.6(2)
C(4)−C(5)−C(10)	179.1(3)	C(18)−C(19)−B(12)	112.4(2)
C(7)−C(6)−B(9)	173.8(3)	C(3)−B(4)−B(5)	104.5(2)
C(6)−C(7)−C(12)	173.3(3)	B(6)−B(5)−B(4)	105.3(2)
C(9)−C(8)−B(13)	175.1(3)	C(4)−B(5)−B(6)	129.2(3)
C(8)−C(9)−C(14)	177.0(3)	C(4)−B(5)−B(4)	125.5(2)
C(11)−C(10)−C(15)	119.6(2)	C(2)−B(6)−B(5)	105.1(2)
C(11)−C(10)−C(5)	120.1(2)	C(17)−B(8)−B(9)	104.9(2)
C(15)−C(10)−C(5)	120.2(2)	C(6)−B(9)−B(8)	130.0(3)
C(10)−C(11)−C(12)	120.3(2)	C(6)−B(9)−B(10)	125.9(3)
C(13)−C(12)−C(11)	119.3(2)	B(8)−B(9)−B(10)	104.1(2)
C(13)−C(12)−C(7)	119.1(2)	C(16)−B(10)−B(9)	106.2(3)
C(11)−C(12)−C(7)	121.6(2)	C(19)−B(12)−B(13)	105.2(3)
C(12)−C(13)−C(14)	121.4(2)	C(8)−B(13)−B(12)	127.9(3)
C(15)−C(14)−C(13)	118.7(2)	C(8)−B(13)−B(14)	127.4(3)
C(15)−C(14)−C(9)	121.5(2)	B(12)−B(13)−B(14)	104.7(2)
C(13)−C(14)−C(9)	119.8(2)	C(18)−B(14)−B(13)	105.1(3)
C(14)−C(15)−C(10)	120.7(2)		

In summary, the electrochemical data demonstrate that in polycobaltacarboranes containing seven-vertex CoC_2B_4 units linked via conjugated carbon chains attached to B(5) or B(7), small but measurable electronic communication between the cobalt centers is observed. Not surprisingly, this effect is particularly enhanced in the triple-decker species **16** and **21**, which incorporate the planar C_2B_3 bridging ring. As previously discussed for the iron analogues and supported by calculations,[5] the C_2B_3 unit appears to make a major contribution to the frontier orbitals of its η^5-coordinated metal complexes.

Experimental Section

Instrumentation. ^1H (500 MHz (where noted), 300 MHz), ^{13}C (125.8 MHz (where noted), 75.4 MHz), and ^{11}B (96.4 MHz) NMR spectra were recorded on GN-300/44 and Varian Unity/Inova 500/51 and 300/51 instruments. ^1H and ^{13}C shifts are referenced to residual ^1H and ^{13}C signals in the deuterated solvent. ^{11}B NMR resonances are referenced to the external standard $BF_3{\cdot}OEt_2$. Unit-resolution mass spectra were acquired on a Finnigan (Model LCQ Classic) quadrupole ion trap mass spectrometer using an atmospheric pressure chemical ionization interface. Infrared spectra were obtained on a Nicolet Impact-400 spectrophotometer. Ultraviolet−visible spectra were recorded on an HP 8452A diode array spectrophotometer or a Cary 5E UV−vis−near-IR spectrophotometer. Elemental analyses were performed by Atlantic Microlabs in Norcross, GA, for new compounds reported, excluding some synthetic intermediates.

Materials and Procedures. All reactions were carried out in oven glassware under a dinitrogen atmosphere using conventional glovebox or Schlenk techniques, and the products were worked up in air. All commercial reagents were used as received without further purification. THF, diethyl ether, and toluene were distilled from sodium benzophenone ketyl prior to use. Triethylamine was distilled from CaH_2 under an inert atmosphere. When anhydrous dichloromethane was required, the solvent was distilled from P_2O_5 under N_2. $Cp^*Co(2,3\text{-}Et_2C_2B_4H_3\text{-}7\text{-}Br)$ (**3a**),[20] $Cp^*Co(2,3\text{-}Et_2C_2B_4H_3\text{-}7\text{-}I)$ (**3b**),[20] $Cp^*Co(2,3\text{-}Et_2C_2B_4H_3\text{-}5\text{-}I)$ (**10**),[21] *nido*-$Cp^*Co(2,3\text{-}Et_2C_2B_3H_4\text{-}5\text{-}I)$ (**13**),[22] 1,3,5-triiodobenzene,[8f] $(Cp^*CoCl)_2$,[23] and $Me_3SiC{\equiv}CI$[24] were prepared according to published procedures.

$C_6H_4O_2BC{\equiv}CSi(CH_3)_3$ (2-((Trimethylsilyl)ethynyl)-1,3,2-benzodioxaborole). To a solution of 5.50 g of $(CH_3)_3SiC{\equiv}CSnMe_3$ (21.1 mmol)[25] in 40 mL of toluene was added 3.3 g of $C_6H_4O_2BCl$ (21.4 mmol) in 80 mL of toluene at −78 °C. The mixture was warmed to room temperature over 7 h and stirred for an additional 12 h. The solvent was removed in vacuo to give a light yellow liquid which was purified by distillation (62 °C, 0.12 mmHg) to give a colorless liquid (3.9 g, 86%). ^1H NMR ($CDCl_3$): δ 0.28 (s, 9H, $SiMe_3$), 7.11−7.14 (m, 2H, C_6H_4), 7.23−7.26 (m, 2H, C_6H_4). $^{13}C\{^1H\}$ NMR (125.75 MHz, $CDCl_3$): δ −0.7 ($Si(CH_3)_3$), 65.9 ($C{\equiv}C$), 112.5 (C_6H_4), 123.1 (C_6H_4), 147.5 (C_6H_4). ^{11}B NMR ($CDCl_3$): δ 23.1 (s). CI^+-mass: *m*/*z* (%) 216.0 ([M^+], 100).

$Cp^*Co[2,3\text{-}Et_2C_2B_4H_3\text{-}7\text{-}C{\equiv}CSi(CH_3)_3]$ (2). Method A. 1 (632 mg, 2.01 mmol) in 40 mL of toluene at 0 °C was treated with *tert*-butyllithium (2.5 mL of a 1.65 M solution in hexane, 4.02 mmol). The solution turned dark red-orange as it was warmed to room temperature; the stirring was continued for over 6 h. Then the mixture was cooled to 0 °C, and $C_6H_4O_2BC{\equiv}CSi(CH_3)_3$ (0.97 g, 4.49 mmol) in 10 mL of toluene was added at 0 °C. The mixture was warmed to room temperature and stirred for an additional 24 h, after which the toluene was removed in vacuo. The residue was taken up in CH_2Cl_2 and washed through 3 cm of silica with CH_2Cl_2. The CH_2Cl_2 wash was column-chromatographed on silica in hexane to recover 62 mg of starting material and was then flash-chromatographed in 1:1 CH_2Cl_2/hexane to afford 615 mg of pure product as an orange red, air-stable crystalline solid (72.9% yield, 80.7% based on the starting complex consumed).

Method B. To (trimethylsilyl)acetylene (73 mg, 0.75 mmol) in 4 mL of THF was added *n*-BuLi (0.5 mL of a 1.51 M solution in hexane, 0.75 mmol) at 0 °C. After the mixture was stirred for 0.5 h, anhydrous $ZnCl_2$ (102 mg, 0.75 mmol) in 2 mL of

---

[20] Curtis, M. A.; Sabat, M.; Grimes, R. N. *Inorg. Chem.* **1996**, *35*, 6703.

[21] Stockman, K. E.; Garrett, D. L.; Grimes, R. N. *Organometallics* **1995**, *14*, 4661.

[22] Piepgrass, K. W.; Stockman, K. E.; Sabat, M.; Grimes, R. N. *Organometallics* **1992**, *11*, 2404.

[23] Koelle, U.; Fuss, B.; Belting, M.; Raabe, E. *Organometallics* **1986**, *5*, 980.

[24] Amatore, C.; Blart, E.; Genet, J. P.; Jutand, A.; Lemaire-Audoire, S.; Savignac, M. *J. Org. Chem.* **1995**, *60*, 6829.

[25] Prepared according to the procedure given for $(CH_3)_3SiC{\equiv}CSnBu_3$ in: Logue. M. W.; Teng. K. *J. Org. Chem.* **1982**, *47*, 2549.

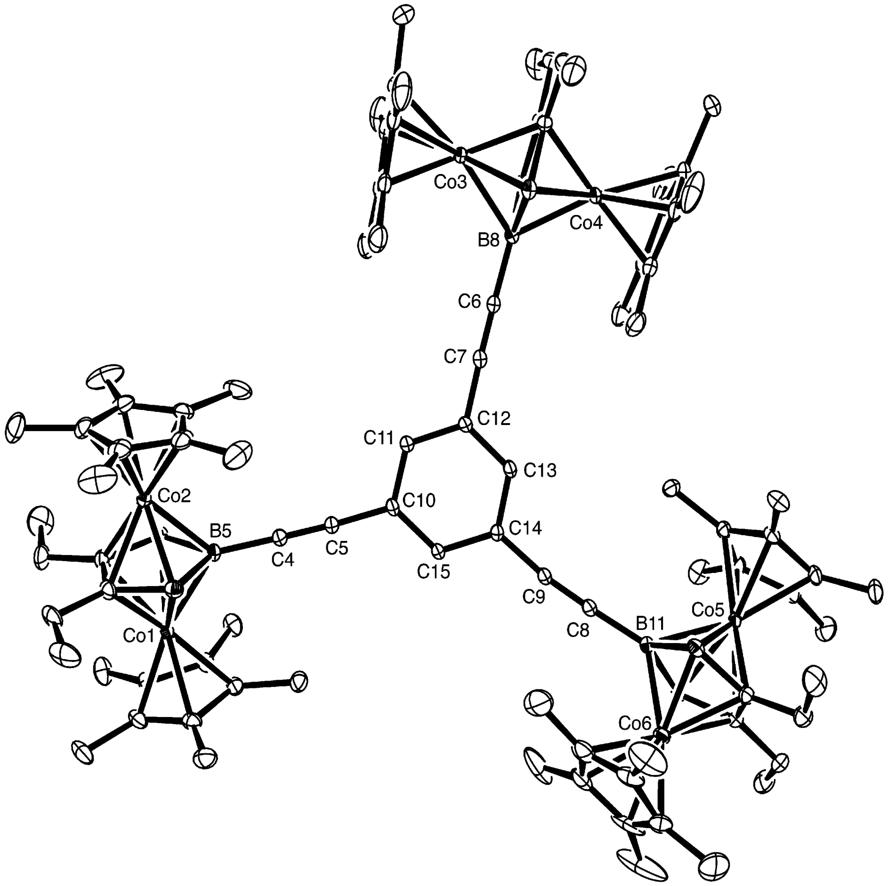

Figure 3. Ortep diagram of 1,3,5-[$Cp^*_2Co_2(2,3\text{-}Et_2C_2B_3H_2\text{-}5\text{-}C{\equiv}C)]_3C_6H_3$ (**21**) (hydrogens omitted).[4a]

Table 4. Formal Electrode Potentials (in V, vs SCE) and Peak-to-Peak Separations (in Parentheses, in mV; Measured at 0.2 V s^{-1}) for Complexes 8, 16, 17, and 19−22

compd	$E°'_{3+/2+}$	$E°'_{2+/+}$	$E°'_{+/0}$	$E''_{0/-}$	$E°'_{-/2-}$	$E°'_{2-/3-}$	solvent
Mononuclear Complexes							
nido-$Cp^*Co(Et_2C_2B_3H_5)$			+0.98[a]				CH_2Cl_2
$Cp^*Co(Et_2C_2B_4H_4)$			+1.16 (100)				CH_2Cl_2
Binuclear Complexes							
8			+1.37[a,b]	−1.82 (120)	−1.94 (120)		THF
17		+1.50[a,b]	+1.18[b,c]	−1.69[b]	−1.74[b]		THF
		+1.48[a,b]	+1.15[c] (100)	−1.77 (50)	−1.83 (70)		CH_2Cl_2
16			+0.36 (80)	−1.81 (70)	−2.80[a,b]		THF
		+1.38[a,b]	+0.12 (100)				CH_2Cl_2
Trinuclear Complexes							
22			+1.36[a,b,d]	−1.95 (100)	−2.10 (100)	−2.20 (100)	THF
	+1.32 (70)	+1.20 (70)	+1.04 (70)				CH_2Cl_2
19			+1.34[a,b,d]	−1.80[d] (100)			THF
		+1.15[c,e] (80)	+1.05[c] (80)				CH_2Cl_2
21			+0.32 (120)	−1.82 (70)	−2.80[a,b]		THF
		+1.40[a,b]	+0.17[d,f] (230)				CH_2Cl_2
20				−0.80[c,g,d]			THF
FcH			+0.53 (100)				THF
			+0.39 (70)				CH_2Cl_2

[a] Peak potential values for irreversible processes. [b] Value estimated by differential pulse voltammetry. [c] Complicated by following reactions. [d] Three-electron process. [e] Two-electron process. [f] Square wave measurement can be simulated with three sequential peaks at +0.26, +0.18, and +0.09 V: see text. [g] Square wave measurement can be simulated with three peaks at +0.7, +0.8, and +1.0 V: see text.

THF was added at 0 °C, the mixture was stirred at room temperature for 2 h, and **3a** (100 mg, 0.25 mmol) and $Pd(PPh_3)_4$ (14 mg, 0.013 mmol) were added. The mixture was refluxed for 4.5 days, after which the solvent was removed in vacuo and the residue was flash chromatographed through 3 cm of silica gel in 1:1 hexane/CH_2Cl_2 to give one orange band. Removal of solvent gave 85 mg (81%) of orange-red product.

Method C. Using a procedure analogous to that described for method B, (trimethylsilyl)acetylene (570 mg, 5.73 mmol) was deprotonated with 5.73 mmol of *n*-BuLi (3.8 mL of a 1.51 M hexane solution) in 20 mL of THF. After the mixture was stirred for 0.5 h, anhydrous $ZnCl_2$ (781 mg, 5.73 mmol) in 20 mL of THF was added at 0 °C. The mixture was stirred at room temperature for 2 h, and **3b** (860 mg, 1.91 mmol) and $Pd(PPh_3)_4$ (110 mg, 0.1 mmol) were added. The mixture was refluxed for 4.5 days, after which the solvent was removed in vacuo and the residue was flash-chromatographed through 5 cm of silica gel in 1:1 hexane/CH_2Cl_2 to give one orange band. Removal of solvent gave 755 mg (94%) of the orange-red product. ^1H NMR ($CDCl_3$): δ −0.04 (s, 9H, $SiMe_3$), 1.35 (t, 6H,

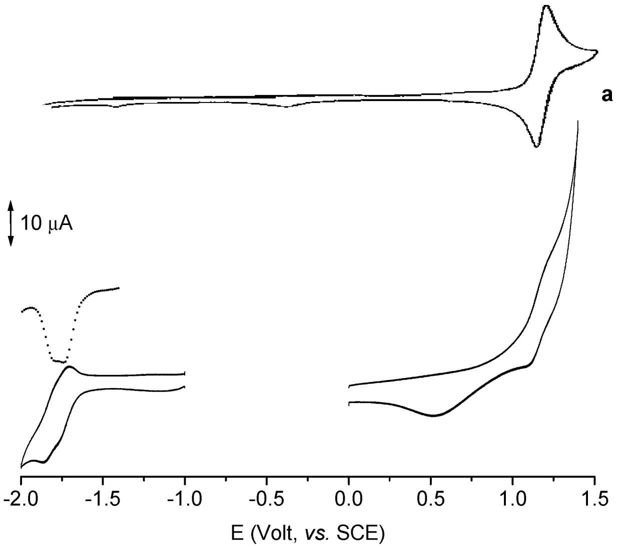

Figure 4. Cyclic (—) and differential pulse (- - -) voltammetric responses recorded at a platinum electrode on CH_2Cl_2 solutions of (a) $Cp^*Co^{III}(Et_2C_2B_4H_4)$ (1.5×10^{-3} mol dm^{-3}) and (b) **17** (0.9×10^{-4} mol dm^{-3}). $[NBu_4][PF_6]$ (0.2 mol dm^{-3}) was used as supporting electrolyte; scan rates were 0.2 and 0.02 V s^{-1}, respectively.

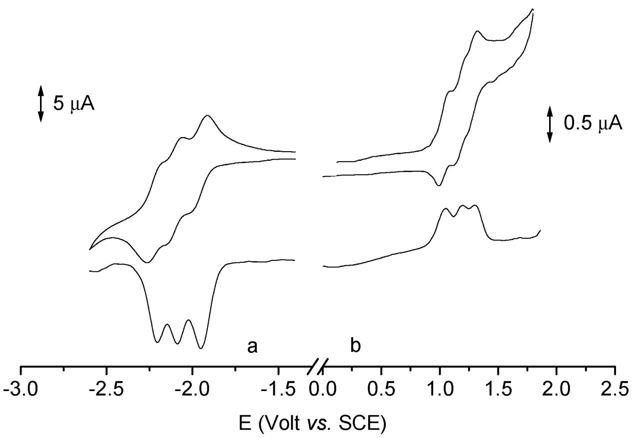

Figure 5. Cyclic (top) and differential pulse (bottom) voltammetric responses of complex **22** recorded under the following experimental conditions: (a) concentration 0.9×10^{-4} mol dm^{-3}, mercury working electrode, thf solution, $[NBu_4][PF_6]$ (0.2 mol dm^{-3}) supporting electrolyte, scan rates 0.2 and 0.02 V s^{-1}, respectively; (b) concentration 0.2×10^{-4} mol dm^{-3}, platinum working electrode, CH_2Cl_2 solution, $[NBu_4][B(C_6F_5)_4]$ (0.05 mol dm^{-3}) supporting electrolyte, scan rate 0.02 V s^{-1}.

J = 7.5 Hz, ethyl CH_3), 1.77 (s, 15H, C_5Me_5), 2.30, 2.46 (sextet, 2H, *J* = 7.5 Hz, ethyl CH_2). $^{13}C\{^1H\}$ NMR ($CDCl_3$): δ −0.4 ($SiMe_3$), 10.0 (C_5Me_5), 14.3 (ethyl CH_3), 22.0 (ethyl CH_2), 90.9 (C_5Me_5), 92.0 ($C{\equiv}CSiMe_3$), 93.4 (C_2B_4). ^{11}B NMR ($CDCl_3$): δ −3.9 (s, 1B), 3.7 (d, 2B, unresolved), 11.9 (d, 1B, unresolved). IR (KBr pellet, cm^{-1}): ν 2969.4 (vs), 2931.8 (s), 2872.4 (m), 2522.1 (vs, B−H), 2126.1 (w, C≡C), 1472.0 (m), 1452.2 (m), 1377.2 (s), 1247.4 (s), 1168.4 (w), 1140.9 (s), 1111.3 (m), 1062.8 (m), 1026.7 (m), 857.8 (vs), 814.0 (vs), 760.1 (m), 696.8 (w). CI$^+$-mass: *m/z* (%) 420.4 ([M$^+$], 100).

Cp*Co(2,3-Et$_2$C$_2$B$_4$H$_3$-7-C≡CH) (4). Compound **2** (630 mg, 1.5 mmol) was dissolved in 30 mL of dry THF, and to this solution was added dropwise 1.5 mL (1.5 mmol of a 1.0 M solution) of tetrabutylammonium fluoride in THF at 0 °C. The reaction mixture was stirred at 0 °C for 40 min, after which the THF was removed and the residue was flash-chromatographed through 3 cm of silica gel in CH_2Cl_2 to give the product as an orange-red solid (510 mg, 98%). ^1H NMR ($CDCl_3$): δ 1.36 (t, 6H, *J* = 7.5 Hz, ethyl CH_3), 1.62 (s, 1H, C≡CH), 1.78 (s, 15H, C_5Me_5), 2.27, 2.46 (sestet, 2H, *J* = 7.5 Hz, ethyl CH_2). $^{13}C\{^1H\}$ NMR ($CDCl_3$): δ 10.0 (C_5Me_5), 14.5 (ethyl CH_3), 21.9 (ethyl, CH_2), 76.6 (C≡CH), 91.0 (C_5Me_5), 93.1 (C_2B_4). ^{11}B NMR ($CDCl_3$): δ −4.5 (s, 1B), 3.4 (d, 2B, J_{BH} = 152 Hz), 11.8 (d, 1B, J_{BH} = 151 Hz). IR (KBr pellet, cm^{-1}): ν 3288.0 (vs, C≡CH), 2971.7 (s), 2962.2 (s), 2932.1 (m), 2964.3 (s), 2875.4(m), 2561.0 (vs, B−H), 2522.8 (vs, B−H), 2059.1 (w, C≡C), 1476.2 (s), 1453.2 (s), 1376.6 (s), 1325.0 (w), 1098.2 (w), 1024.5 (s), 914.5 (w), 815.0 (s), 789.7 (s), 671.8 (vs), 633.7 (s), 648.8 (vs), 430.9 (m). CI$^+$-mass: *m/z* (%) = 347.4 ([M$^+$ − 1], 100).

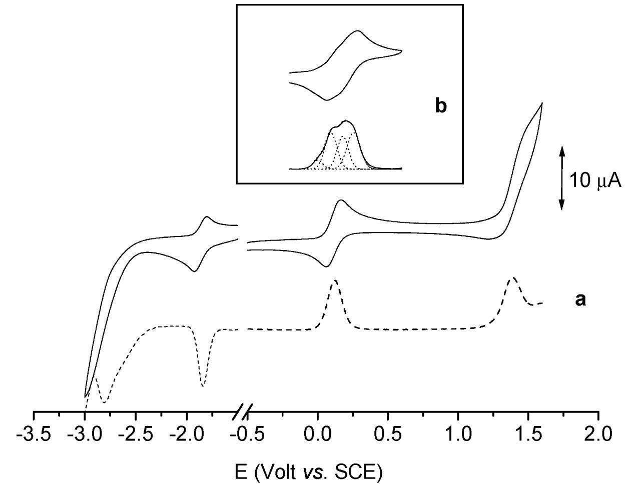

Figure 6. Comparison between the voltammetric behaviors of **16** and **21** (inset). (a) Anodic processes: cyclic (—) and Osteryoung square wave (- - -) voltammetric responses recorded at a gold electrode on a thf solution of **16** (0.4×10^{-3} mol dm^{-3}). $[NBu_4][PF_6]$ (0.2 mol dm^{-3}) was used as supporting electrolyte; scan rates were 0.2 and 0.1 V s^{-1}, respectively. Cathodic processes: cyclic (—) and Osteryoung square wave (- - -) voltammetric responses recorded at a platinum electrode on a CH_2Cl_2 solution of **16** (0.4×10^{-3} mol dm^{-3}). $[NBu_4][PF_6]$ (0.2 mol dm^{-3}) was used as supporting electrolyte; scan rates were 0.2 and 0.1 V s^{-1}, respectively. (b) Cyclic (top) and Osteryoung square wave (bottom) voltammetric responses recorded at a platinum electrode on a CH_2Cl_2 solution of **21** (0.7×10^{-3} mol dm^{-3}) (- - -, simulated Gaussian curve). $[NBu_4][B(C_6F_5)_4]$ (0.1 mol dm^{-3}) was used as supporting electrolyte; the scan rate was 0.2 V s^{-1}.

Cp*Co[2,3-Et$_2$C$_2$B$_4$H$_3$-7-(C$_2$HCo$_2$(CO)$_6$] (5). Compound **4** (30 mg, 0.09 mmol) in 4 mL of pentane was slowly added to a 5 mL solution of $Co_2(CO)_8$ (30 mg, 0.09 mmol) in pentane. After the mixture was stirred for 3 days at room temperature, the solvent was removed and the reaction mixture was separated on silica TLC plates to afford a red-brown solid (48 mg, 88%). ^1H NMR ($CDCl_3$): δ 1.36 (t, 6H, *J* = 7.5 Hz, ethyl CH_3), 5.70 (s, 1H, C−CH), 1.79 (s, 15H, C_5Me_5), 2.11, 2.43 (sextet, 2H, *J* = 7.8 Hz, ethyl CH_2). $^{13}C\{^1H\}$ NMR ($CDCl_3$): δ 10.2 (C_5Me_5), 14.5 (ethyl CH_3), 21.8 (ethyl CH_2), 91.0 (C_5Me_5), 94.0 (C_2B_4), 199.9 (C−O). ^{11}B NMR ($CDCl_3$): δ 4.6 (unresolved, BH, 3B), 12.6 (s, 1B). IR (KBr pellet, cm^{-1}): ν 2964.7 (m), 2914.0 (s), 2873.5 (m), 2545.3 (m, B−H), 2534.1 (s, B−H), 2515.4 (s, B−H), 2087.81 (vs, C−C), 2005.4 (vs, C−O), 1496.6 (s), 1446.3 (m), 1433.1 (m), 1059.6 (w), 1020.5 (m), 812.8 (s), 618.0 (w), 562.1 (s), 515.6 (vs), 498.3 (s), 480.0 (m). UV−vis (CH_2Cl_2, nm (%)): 308 (100), 428 (5) ϵ_{max} = 34 493 cm^{-1} M^{-1}. Anal. Calcd for $B_4C_{24}Co_3H_{29}O_6$: C, 45.50; H, 4.61. Found: C, 45.80; H, 4.69.

Cp*Co(2,3-Et$_2$C$_2$B$_4$H$_2$-5-I-7-C≡CC≡CSiMe$_3$) (6). To compound **4** (139 mg, 0.4 mmol) in 15 mL of THF was added *t*-BuLi (0.2 mL of a 2.05 M solution in hexane, 0.4 mmol) at 0 °C. After 0.5 h of stirring at 0 °C, anhydrous $ZnCl_2$ (54.5 mg, 0.4 mmol) in 5 mL of THF was added at 0 °C. The mixture was stirred at room temperature for 2 h, and $Me_3SiC\equiv CI$ (450 mg, 1.6 mmol) and $Pd(PPh_3)_4$ (23 mg, 0.02 mmol) were added. The mixture was refluxed for 2 days, after which the solvent was removed in vacuo. The residue was taken up in hexane, and the residue was flash-chromatographed through 3 cm of silica gel in hexane followed by CH_2Cl_2. Column chromatography of the CH_2Cl_2 wash in 1:1 hexane/CH_2Cl_2 afforded **6** as a major orange-red band (103 mg, 45.2%); chromatography of the above CH_2Cl_2 wash in 1:2 hexane/CH_2Cl_2 afforded the known byproduct $Cp^*Co(2,3\text{-}Et_2C_2B_4H_2\text{-}5\text{-}I\text{-}7\text{-}C\equiv CH)$[1] as an orange-yellow band (55 mg, 29%). ^1H NMR ($CDCl_3$): δ 0.11 (s, 9H, $SiMe_3$), 1.32 (t, 6H, $J = 7.5$ Hz, ethyl CH_3), 1.76 (s, 15H, C_5Me_5), 2.29, 2.46 (sextet, 2H, $J = 7.5$ Hz, ethyl CH_2). $^{13}C\{^1H\}$ NMR ($CDCl_3$): δ −0.6 ($SiMe_3$), 9.6 (C_5Me_5), 14.7 (ethyl CH_3), 21.6 (ethyl CH_2), 91.9 (C_5Me_5), 95.6 (C_2B_4), 92.1($C\equiv C$), 84.2 ($C\equiv C$), 89.2 ($C\equiv C$). ^{11}B NMR ($CDCl_3$): δ −6.4 (unresolved, BH, 1B), 4.1(unresolved, BH, 3B). IR (KBr pellet, cm^{-1}): ν 2969.6 (s), 2928.8 (m), 2911.5 (m), 2871.2 (w), 2533.5 (vs, B−H), 2186.6 (w, $C\equiv C$), 2080.4 (vs, $C\equiv C$), 1471.7 (m), 1451.1 (m), 1383.5 (m), 1375.8 (s), 1249.7 (s), 1222.4 (w), 1064.3 (w), 1029.8 (m), 933.0 (m), 842.0 (vs), 799.3 (s), 759.8 (m), 653.2 (m). CI^+-mass: m/z (%) 571.3 ($[M^+] + 1$, 100).

$Cp^*Co(2,3\text{-}Et_2C_2B_4H_2\text{-}5\text{-}I\text{-}7\text{-}C\equiv CC\equiv CH)$ (7). Compound **6** (160 mg, 0.28 mmol) was desilylated with 0.28 mL of a 1.0 M TBAF solution (0.28 mmol) in 8 mL of dry THF. The reaction mixture was stirred at 0 °C for 1 h, after which the THF was removed and the residue was flash-chromatographed through 3 cm of silica gel in CH_2Cl_2 to give one orange-red band. Removal of solvent gave an orange-red solid (126 mg, 90.5%). ^1H NMR ($CDCl_3$): δ 1.33 (t, 6H, $J = 7.5$ Hz, ethyl CH_3), 1.94 (s, 1H, $C\equiv CH$), 1.77 (s, 15H, C_5Me_5), 2.31, 2.48 (sextet, 2H, $J = 7.8$ Hz, ethyl CH_2). $^{13}C\{^1H\}$ NMR (125.75 MHz, $CDCl_3$): δ 9.6 (C_5Me_5), 14.7 (ethyl CH_3), 21.6 (ethyl CH_2), 65.0 ($C\equiv C$), 69.3 ($C\equiv C$), 92.0 (C_5Me_5), 95.5 (C_2B_4). ^{11}B NMR ($CDCl_3$): δ −6.3 (s, 1B), 4.1 (unresolved, BH, 3B). IR (KBr pellet, cm^{-1}): ν 3255.7 (vs, $C\equiv CH$), 2975.3 (m), 2906.8 (w), 2557.4 (s, B−H), 2196.9 (w, $C\equiv C$), 2046.2 (m, $C\equiv C$), 1472.0 (m), 1452.1 (m), 1382.9 (vs), 1195.5 (m), 1018.7 (m), 780.0 (s), 650.4 (s). CI^+-mass: m/z (%) 499.2 ($[M^+] + 1$, 100). Anal. Calcd for $B_4C_{20}CoH_{28}I$: C, 48.28; H, 5.67. Found: C, 48.05; H, 5.58.

$[Cp^*Co(2,3\text{-}Et_2C_2B_4H_3\text{-}7\text{-}C\equiv C)]_2$ (8). A mixture of cupric chloride (16 mg, 0.16 mmol) and **4** (20 mg, 0.081 mmol) was dissolved in a mixture of 6 mL of toluene and 1 mL of pyridine. The solution was stirred in the open air at 100 °C for 20 h, solvent was removed in vacuo, and the residue was flash-chromatographed through 3 cm of silica gel in CH_2Cl_2 to give one orange band. Removal of solvent gave an orange solid product, which was purified by thick-layer chromatography on silica gel in 2:1 CH_2Cl_2/hexane to afford orange-red crystalline **8** (14 mg, 70%). ^1H NMR ($CDCl_3$): δ 1.25 (t, 12H, $J = 7.5$ Hz, ethyl CH_3), 1.73 (s, 30H, C_5Me_5), 2.17, 2.36 (sextet, 4H, $J = 7.5$ Hz, ethyl CH_2). $^{13}C\{^1H\}$ NMR ($CDCl_3$): δ 10.0 (C_5Me_5), 14.6 (ethyl CH_3), 21.8 (ethyl CH_2), 73.8 ($C\equiv C$), 93.7 ($C\equiv C$), 91.0 (C_5Me_5), 92.1 (C_2B_4). ^{11}B NMR ($CDCl_3$): δ −4.1 (s, 2B), 4.6 (unresolved, BH, 4B), 4.3 (unresolved, BH, 2B). IR (KBr pellet, cm^{-1}): ν 2963.4 (s), 2911.0 (m), 2872.9 (m), 2547.1 (vs, B−H), 2094.4 (m, $C\equiv C$), 1476.4 (m), 1452.0 (m), 1377.0 (s), 1130.9 (m), 1103.1 (m), 1072.3 (m), 1061.5 (m), 1025.9 (s), 803.1 (vs), 790.6 (vs), 643.2 (w), 588.5 (w). UV−vis (CH_2Cl_2, nm (%)): 312 (100), 231 (55), 251 (31), 421 (3), $\epsilon_{max} = 84\,240\ cm^{-1}\ M^{-1}$. CI^+-mass: m/z (%) 694.0 ($[M^+]$, 100).

$Cp^*Co(2,3\text{-}Et_2C_2B_4H_3\text{-}7\text{-}C_6H_4COOH)$ (9). To a mixture of **4** (70 mg, 0.2 mmol), $Pd(PPh_3)_2Cl_2$ (7 mg, 0.01 mmol), CuI (4 mg, 0.02 mmol), and 1,4-IC_6H_4COOH (50 mg, 0.2 mmol) were added 4 mL of THF and 1 mL of Et_3N. The mixture was stirred for 18 h, after which the solvent was removed in vacuo. The residue was dissolved in 6 mL of CH_2Cl_2, 1 mL of 10% HCl was added, and the mixture was stirred for 20 min, after which it was washed with 5 mL of H_2O followed by three 6 mL portions of saturated NaCl solution and finally was dried over anhydrous Na_2SO_4. Removal of the solvent afforded 70 mg of **9** as an orange-red solid (75%). ^1H NMR (500 MHz, $CDCl_3$): δ 1.39 (t, 6H, $J = 7.5$ Hz, ethyl CH_3), 1.80 (s, 45H, C_5Me_5), 2.35, 2.52 (sextet, 6H, $J = 7.5$ Hz, ethyl CH_2), 7.28 (d, 2H, $J = 8$ Hz, C_6H_4), 7.88 (d, 2H, $J = 8$ Hz, C_6H_4). $^{13}C\{^1H\}$ NMR (125.75 MHz, $CDCl_3$): δ 10.1 (C_5Me_5), 14.6 (ethyl CH_3), 22.0 (ethyl CH_2), 87.4 ($C\equiv C$), 91.1 (C_5Me_5), 93.6 (C_2B_4), 129.7 (C_6H_4), 131.6 (C_6H_4), 171.3 (C−O). ^{11}B NMR ($CDCl_3$): δ −2.9 (unresolved, BH, 3B), 3.2 (s, 1B). IR (KBr pellet, cm^{-1}): ν 2970.1 (s), 2930.8 (m), 2909.3 (w), 2535.7 (vs, B−H), 1693.5 (s), 1602.6 (vs), 1538.1 (w), 1452.2 (w), 1404.0 (m), 1382.5 (vs), 1309.2 (m), 1265.6 (s), 1173.0 (m), 1027.2 (w). CI^+-mass: m/z (%) 469.4 ($[M^+] + 1$, 100). Anal. Calcd for $C_{25}H_{33}O_2Co$: C, 64.20; H, 7.11. Found: C, 64.17; H, 7.20.

$Cp^*Co(2,3\text{-}Et_2C_2B_4H_3\text{-}5\text{-}C\equiv CSiMe_3)$ (11). To (trimethylsilyl)acetylene (340 mg, 3.46 mmol) in 30 mL of THF was added 3.46 mmol of *n*-butyllithium (2.3 mL of a 1.51 M solution in hexane) at 0 °C. After 0.5 h of stirring, anhydrous $ZnCl_2$ (472 mg, 3.46 mmol) in 15 mL of THF was added at 0 °C, the mixture was stirred at room temperature for 2 h, and **10** (520 mg 1.15 mmol) and $Pd(PPh_3)_4$ (66.7 mg, 0.058 mmol) were added. The mixture was refluxed for 4.5 days, after which the solvent was removed in vacuo and the residue was flash-chromatographed through 5 cm of silica gel in 1:1 hexane/CH_2Cl_2 to give one orange band. Removal of solvent gave **11** as an orange-red solid (472 mg, 97%). This complex was prepared earlier in 25% yield (see compound **7** in ref 4c) via attack of lithium (trimethylsilyl)acetylenide at the reduced $Cp^*Co^{II}(2,3\text{-}Et_2C_2B_4H_3\text{-}5\text{-}I)^-$ anion.

$Cp^*Co(2,3\text{-}Et_2C_2B_4H_3\text{-}5\text{-}C\equiv CH)$ (12). Using a procedure analogous to that described above for **7**, 380 mg of **11** (380 mg, 0.905 mmol) was desilylated with a 1.0 M solution of tetrabutylammonium fluoride in THF (0.91 mL of a 1 M solution in THF, 0.91 mmol). The residue was flash-chromatographed through 3 cm of silica gel in CH_2Cl_2 to give one orange band. Removal of solvent gave **12** as an orange-red solid (305 mg, 97%). ^1H NMR ($CDCl_3$): δ 1.17 (t, 6H, $J = 7.5$ Hz, ethyl CH_3), 1.82 (s, 15H, C_5Me_5), 2.29, 2.49 (sextet, 2H, $J = 6.9$ Hz, ethyl CH_2), 3.252 (s, 1H, $C\equiv CH$). $^{13}C\{^1H\}$ NMR ($CDCl_3$): δ 9.4 (C_5Me_5), 14.8 (Et, CH_3), 21.5 (Et, CH_2), 91.0 (C_5Me_5), 92.9 (C_2B_4), 96.3 ($C\equiv CH$). ^{11}B NMR ($CDCl_3$): δ 7.4 (s, 1B), 4.3 (d, 2B, $J_{BH} = 187$ Hz), 1.9 (d, 1B, unresolved). IR (KBr, pellet, cm^{-1}): ν 3289.7 (vs, $C\equiv CH$), 2977.3 (s), 2963.5 (s), 2925.0 (m), 2869.5 (m), 2552.6 (vs, B−H), 2531.9 (vs, B−H), 2519.0 (vs, B−H), 2042.6 (w, $C\equiv C$), 1472.0 (m), 1450.1 (s), 1427.2 (w), 1376.9 (s), 1383.7 (s), 1206.3 (w), 1163.4 (m), 1067.0 (m), 1028.0 (m), 873.9 (m), 862.0 (s), 662.2 (vs), 595.8 (vs), 560.8 (w), 503.6 (w), 448.7 (w). CI^+-mass: m/z (%) 349.4 ($[M^+] + 1$, 100).

$Cp^*Co(2,3\text{-}Et_2C_2B_3H_4\text{-}5\text{-}C\equiv CSiMe_3)$ (14). In a procedure analogous to that described above for **11**, (trimethylsilyl)acetylene (420 mg, 4.1 mmol) was deprotonated with *n*-butyllithium (2.7 mL of a 1.51 M solution in hexane, 4.1 mmol) in 30 mL of THF. The solution was stirred for 0.5 h at 0 °C, and anhydrous $ZnCl_2$ (559 mg, 4.1 mmol) in 15 mL of THF was added at 0 °C. The solution was stirred at room temperature for 2 h, and **13** (600 mg, 1.36 mmol) and $Pd(PPh_3)_4$ (78.6 mg, 0.07 mmol) were added. The mixture was refluxed for 3.5 days, following which the solvent was removed in vacuo and the residue was flash-chromatographed through 3 cm of silica gel in 1:1 hexane/CH_2Cl_2 to give one orange band. Removal of solvent gave **14** as an orange-yellow solid (520 mg, 93%).

$Cp^*Co(2,3\text{-}Et_2C_2B_3H_4\text{-}5\text{-}C\equiv CH)$ (15). Method A. In a procedure analogous to that described above for **7**, compound **14** (175 mg, 0.43 mmol) was desilylated with 0.43 mL of a 1.0 M TBAF solution (0.43 mmol). Flash chromatography of the product in hexane give one orange-yellow band. Removal of solvent gave **15** as a yellow solid (87 mg, 60%).

Method B. To compound **11** (408 mg, 1.17 mmol) in an open flask was added 6 mL of *N*,*N*,*N*′,*N*′-tetramethylethylenediamine (TMEDA) and ca. 10 drops of water, and the mixture was stirred for 3 h. The TMEDA was removed by vacuum, and the residue was taken up in hexane and flash-chromatographed through 3 cm of silica gel in hexane to give one orange-yellow band. Removal of solvent gave **15** as a yellow solid (360 mg, 90%). ^{1}H NMR (CDCl$_3$): δ −5.15 (2H, B−H−B), 1.09 (t, 6H, J = 7.2 Hz, ethyl CH$_3$), 1.78 (s, 15H, C$_5$Me$_5$), 2.90, 2.12 (sextet, 2H, J = 7.5 Hz, ethyl CH$_2$), 2.91 (s, 1H, C≡CH). ^{13}C{^{1}H} NMR (CDCl$_3$): δ 9.2 (C$_5$Me$_5$), 17.3 (Et, CH$_3$), 22.3 (Et, CH$_2$), 92.4 (C$_5$Me$_5$), 94.5 (C$_2$B$_3$). ^{11}B NMR (CDCl$_3$): δ 6.6 (s, 1B), 0.9(d, 2B, J_{BH} = 138 Hz). IR (KBr, pellet, cm^{-1}): ν 2965.2 (s), 2907.7 (s), 2865.4 (m), 2519.2 (s, B−H), 2495.9 (s, B−H), 2120.1 (m, C≡C), 1896.2, 1873.3, 1843.3 (B−H−B), 1567.8 (m), 1480.4 (m), 1468.6 (m), 1428.6 (m), 1375.8 (s), 1248.8 (s), 1134.3 (m), 1101.0 (s), 1029.7 (s), 893.8 (vs), 853.1 (vs), 772.5 (s), 754.3 (s), 669.6 (s), 582.0 (w), 526.6 (m), 480.7 (w). CI$^+$-mass: m/z (%) 339.5 ([M$^+$] + 1, 100).

Cp*Co(2,3-Et$_2$C$_2$B$_3$H$_2$-5-C≡CSiMe$_3$)CoCp* (16). Compound **14** (220 mg, 0.53 mmol) in 20 mL of THF was deprotonated with *n*-BuLi (0.35 mL of a 1.51 M solution in hexane, 0.53 mmol) at 0 °C. This solution was stirred for 2 h at room temperature, after which (Cp*CoCl)$_2$ (122.6 mg, 0.27 mmol) in 5 mL of THF was added. The mixture was stirred overnight, and the solvent was removed in vacuo. The red-brown residue was washed through 3 cm of silica gel with dichloromethane. The crude material was then chromatographed on a silica gel column in 1:1 hexane/dichloromethane to give one major red-brown band. Removal of solvent afforded **16** as an air-stable dark red solid (120 mg, 37.3%). ^{1}H NMR (CDCl$_3$): δ 0.27 (s, 9H, BC≡CSiMe$_3$), 1.54 (t, 6H, J = 7.5 Hz, ethyl CH$_3$), 1.60 (s, 30H, C$_5$Me$_5$), 2.54 (m, 4H, J = 7.5 Hz, ethyl CH$_2$). ^{13}C{^{1}H} NMR (125.75 MHz, CDCl$_3$): δ 0.6 (BC≡CSiMe$_3$), 9.2 (C$_5$Me$_5$), 15.5 (ethyl CH$_3$), 23.7 (ethyl CH$_2$), 87.4 (C$_5$Me$_5$), 88.3 (C$_2$B$_4$), 126.5 (BC≡CSiMe$_3$). ^{11}B NMR (CDCl$_3$): δ 9.2 (BH, 2B, unresolved), 40.9 (s, 1B). IR (KBr pellet, cm^{-1}): ν 2964.6 (s), 2907.5 (vs), 2483.7 (s, B−H), 2075.9 (s, C≡C), 1476.3 (m), 1447.7 (m), 1376.9 (s), 1241.3 (m), 1153.2 (m), 1100.8 (m), 1021.9 (m), 879.3 (s), 847.2 (vs), 802.0 (vs), 754.7 (m), 690.6 (w), 584.7 (m). UV−vis (CH$_2$Cl$_2$, nm (%)): 312 (100), 231 (55), 251 (31), 421 (3), ϵ_{max} = 84 240 cm^{-1} M^{-1}. CI$^+$-mass: m/z (%) = 603.6 ([M$^+$], 100). Anal. Calcd for B$_3$C$_{31}$Co$_2$H$_{51}$Si: C, 61.84; H, 8.54. Found: C, 61.72; H, 8.55.

[Cp*Co(2,3-Et$_2$C$_2$B$_4$H$_3$-5-C≡C)]$_2$ (17). To a mixture of **12** (347.6 mg, 1 mmol), Pd(PPh$_3$)$_2$Cl$_2$ (18 mg, 0.026 mmol), CuI (9.5 mg, 0.05 mmol), and I$_2$ (127 mg, 0.5 mmol) were added 5 mL of pyridine and 1 mL of Et$_3$N, and the mixture was stirred for 15 h. Solvent was removed in vacuo, and the residue was flash-chromatographed through 5 cm of silica gel in hexane to give one yellow band, which was Cp*Co(2,3-Et$_2$C$_2$B$_3$H$_5$-5-C≡CH (10 mg), then CH$_2$Cl$_2$ to give one orange-red band. Removal of solvent gave the orange-red solid **17** (228 mg, 65.8%). ^{1}H NMR (CDCl$_3$): δ 1.17 (t, 12H, J = 7.5 Hz, ethyl CH$_3$), 1.82 (s, 30H, C$_5$Me$_5$), 2.28, 2.48 (sextet, 4H, J = 7.2 Hz, ethyl CH$_2$). ^{13}C{^{1}H} NMR (125.75 MHz, CDCl$_3$): δ 9.7 (C$_5$Me$_5$), 15.0 (ethyl CH$_3$), 21.7 (ethyl CH$_2$), 92.8 (C≡C), 91.2 (C$_5$Me$_5$), 96.3 (C$_2$B$_4$). ^{11}B NMR (CDCl$_3$): δ 4.3 (unresolved, BH, 6B), 8.2 (unresolved, BH, 2B). IR (KBr pellet, cm^{-1}): ν 2973.1 (s), 2909.7 (s), 2870.2 (m), 2552.1 (vs, B−H), 2074.4 (w, C≡C), 1472.0 (s), 1448.1 (s), 1383.0 (vs), 1376.7 (vs), 1158.5 (s), 1123.4 (m), 1064.5 (m), 1026.8 (s), 884.8 (m), 861.5 (s), 674.6 (m), 592.5 (w), 446.4 (m). UV−vis (CH$_2$Cl$_2$, nm (%)): 289 (100), 350 (71), ϵ_{max} = 38 666 cm^{-1} M^{-1}. CI$^+$-mass: m/z (%) 694.7 ([M$^+$], 100). Anal. Calcd for C$_{36}$H$_{36}$B$_8$Co$_2$: C, 62.38; H, 8.14. Found: C, 62.29; H, 8.14.

[Cp*Co(2,3-Et$_2$C$_2$B$_3$H$_4$-5-C≡C)]$_2$ (18). Triethylamine (121 mg, 1.2 mmol) was added to a stirred mixture of Pd(PPh$_3$)$_4$ (18 mg, 016 mmol), CuI (8.6 mg, 0.045 mmol), and **15** (203 mg, 0.6 mmol) in 4 mL of pyridine. This mixture was then sequentially treated with chloroacetone (56 mg, 0.6 mmol) and stirred for 15 h at room temperature. Following removal of the solvent in vacuo, the residue was flash-chromatographed through 5 cm of silica gel in hexane to give one yellow band, orange-yellow solid **18** (137 mg, 68%). ^{1}H NMR (CDCl$_3$): δ 1.09 (t, 12H, J = 7.5 Hz, ethyl CH$_3$), 1.79 (s, 30H, C$_5$Me$_5$), 1.90, 2.12 (sextet, 4H, J = 7.5 Hz, ethyl CH$_2$), −5.10 (B−H−B, 4H). ^{13}C{^{1}H} NMR (CDCl$_3$): δ 9.3 (C$_5$Me$_5$), 17.2 (ethyl CH$_3$), 22.4 (ethyl CH$_2$), 85.0 (C≡C), 91.5 (C$_2$B$_3$), 92.7 (C$_5$Me$_5$), 111.9 (C≡C). ^{11}B NMR (CDCl$_3$): δ 1.1 (unresolved, 4B), 6.6 (s, 2B). IR (KBr pellet, cm^{-1}): ν 2962.8 (vs), 2928.4 (s), 2906.7 (s), 2868.0 (s), 2520.6 (vs, B−H), 2090.0 (m, C≡C), 1879.6 (m, B−H−B), 1569.7 (s), 1505.6 (m), 1481.6 (s), 1450.7 (s), 1379.8 (vs), 1075.1 (m), 1029.2 (s), 996.2 (m), 879.7 (s), 772.6 (s), 626.4 (w), 440.0 (w). UV−vis (CH$_2$Cl$_2$, nm (%)): 243 (100), 295 (78), ϵ_{max} = 60 751 cm^{-1} M^{-1}. CI$^+$-mass: m/z (%) 674.5 ([M$^+$], 100). Anal. Calcd for C$_{36}$H$_{58}$B$_6$Co$_2$: C, 64.19; H, 8.68. Found: C, 64.24; H, 8.72.

{Cp*Co(2,3-Et$_2$C$_2$B$_4$H$_3$-5-C≡C)}$_3$C$_6$H$_3$ (19). To a mixture of **12** (70 mg, 0.1 mmol), Pd(PPh$_3$)$_2$Cl$_2$ (7 mg, 0.01 mmol), CuI (4 mg, 0.02 mmol), and C$_6$H$_3$I$_3$ (27 mg, 0.06 mmol) were added 5 mL of THF and 5 mL of Et$_3$N. The mixture was stirred for 3 days, after which the solvent was removed in vacuo. The residue was taken up in CH$_2$Cl$_2$ and flash-chromatographed through 3 cm of silica gel in CH$_2$Cl$_2$. TLC column chromatography of the CH$_2$Cl$_2$ wash with 1:3 hexane/CH$_2$Cl$_2$ afforded **19** as a major orange-yellow band (40 mg, 60%). ^{1}H NMR (CDCl$_3$): δ 1.19 (t, 18H, J = 7.5 Hz, ethyl CH$_3$), 1.85 (s, 45H, C$_5$Me$_5$), 2.31, 2.51 (sextet, 6H, J = 7.2 Hz, ethyl CH$_2$), 7.53 (s, 3H, C$_6$H$_4$). ^{13}C{^{1}H} NMR (125.75 MHz, CDCl$_3$): δ 9.7 (C$_5$Me$_5$), 15.0 (ethyl CH$_3$), 21.7 (ethyl CH$_2$), 91.2 (C$_5$Me$_5$), 93.1 (C$_2$B$_4$), 110.3 (C≡C), 125.9 (C$_6$H$_4$), 131.8 (C$_6$H$_4$). ^{11}B NMR (at 50 °C, CDCl$_3$): δ 8.7 (s, 3B), 4.1 (BH, 9B, unresolved). IR (KBr pellet, cm^{-1}): ν 2965.3 (s), 2931.0 (m), 2870.6 (w), 2540.7 (vs, B−H), 2161.8 (w, C≡C), 1572.5 (s), 1378.1 (m), 1238.4 (m), 1025.8 (m), 869.7 (s), 683.7 (m). UV−vis (CH$_2$Cl$_2$, nm (%)): 299 (100), 271 (89), ϵ_{max} = 284 699 cm^{-1} M^{-1}. CI$^+$-mass: m/z (%) 1116.9 ([M$^+$], 100).

{Cp*Co(2,3-Et$_2$C$_2$B$_3$H$_4$-5-C≡C)}$_3$C$_6$H$_3$ (20). To a mixture of **15** (318 mg, 0.94 mmol), Pd(PPh$_3$)$_2$Cl$_2$ (33 mg, 0.05 mmol), CuI (18 mg, 0.1 mmol), and C$_6$H$_3$I$_3$ (137 mg, 0.3 mmol) were added 5 mL of THF and 1 mL of Et$_3$N. The mixture was stirred for 4 h, after which the solvent was removed in vacuo and the residue was taken up in CH$_2$Cl$_2$ and flash-chromatographed through 3 cm of silica gel in CH$_2$Cl$_2$. Column chromatography of the residue from the CH$_2$Cl$_2$ wash in hexane gave **20** as a major orange-yellow band (283 mg, 87%). ^{1}H NMR (CDCl$_3$): δ 1.11 (t, 18H, J = 7.8 Hz, ethyl CH$_3$), 1.81 (s, 45H, C$_5$Me$_5$), 1.93, 2.15 (sextet, 6H, J = 7.5 Hz, ethyl CH$_2$), 7.48 (s, 3H, C$_6$H$_4$), −4.96 (6H, B−H−B). ^{13}C{^{1}H} NMR (CDCl$_3$): δ 9.3 (C$_5$Me$_5$), 17.3 (ethyl CH$_3$), 22.4 (ethyl CH$_2$), 105.4 (C≡C), 92.6 (C$_5$Me$_5$), 111.9 (C$_2$B$_3$), 124.9 (C$_6$H$_4$), 132.9 (C$_6$H$_4$). ^{11}B NMR (CDCl$_3$): δ 6.5 (s, 3B), 0.6 (BH, 6B, unresolved). IR (KBr pellet, cm^{-1}): ν 3055.2 (w), 2960.3 (vs), 2962.3 (s), 2866.7 (m), 2509.9 (vs, B−H), 2181.0 (w, C≡C), 1576.2 (vs), 1560.2 (m), 1376.5 (s), 1202.8 (s), 1027.8 (m), 932.2 (m), 875.9 (s), 773.8 (m). UV−vis (CH$_2$Cl$_2$, nm (%)): 274 (100), 328 (17) ϵ_{max} = 32 392 cm^{-1} M^{-1}. CI$^+$-mass: m/z (%) 1085.7 ([M$^+$], 100). Anal. Calcd for B$_9$C$_{60}$Co$_3$H$_{90}$: C, 66.39; H, 8.36. Found: C, 66.63; H, 8.39.

1,3,5-[Cp*$_2$Co$_2$(2,3-Et$_2$C$_2$B$_3$H$_2$-5-C≡C)]$_3$C$_6$H$_3$ (21). To an 84 mg (0.077 mmol) sample of **20** in 8 mL of THF was added 11 mg of NaH (0.46 mmol) at room temperature. This solution was stirred for 1 h, 53 mg (0.12 mmol) of (Cp*CoCl)$_2$[11] in 5 mL of THF was added, and the mixture was stirred overnight, after which the solvent was removed in vacuo. The red-brown residue was washed through 3 cm of alumina with dichloromethane, and the crude material was chromatographed on alumina TLC in 1:1 hexane/dichloromethane to afford **21** as an air-stable dark red solid (88 mg, 0.053 mmol, 69% yield). ^{1}H NMR (300 MHz, 25 °C, CDCl$_3$): δ 1.57 (t, 6H, J = 7.2 Hz, ethyl CH$_3$), 1.67 (s, 30H, C$_5$Me$_5$), 2.53−2.60 (q, 4H, J = 7.5 Hz, ethyl CH$_2$), 7.61 (s, 3H, C$_6$H$_4$). ^{13}C{^{1}H} NMR (75.5 MHz, 25 °C, CDCl$_3$): δ 9.4 (C$_5$Me$_5$), 15.6 (ethyl CH$_3$), 23.9 (ethyl CH$_2$), 87.6 (C$_5$Me$_5$), 88.1 (C$_2$B$_4$), 122.8 (BC≡C), 127.1 (C$_6$H$_4$), 129.1 (C$_6$H$_4$). ^{11}B NMR (96.4 MHz, 25 °C, CDCl$_3$): δ 8.6 (BH, 2B, unresolved), 41.5 (s, 1B); IR (KBr pellet, cm^{-1}): ν 2974.2 (m), 2903.7 (vs), 2471.7 (s, B−H), 2131.7 (w, C≡C), 1569.7 (m), 1560.2 (m), 1458.6 (m), 1457.0 (m), 1379.4 (s), 1212.3 (w), 1079.5 (w), 1025.7 (m), 960.3 (w), 803.5 (s). UV−vis (CH_2Cl_2, nm (%)): 243 (100), 276 (68), 345 (98), 428 (31), 528 (8), 753 (10), $\epsilon_{max} = 74\ 074\ cm^{-1}\ M^{-1}$. CI^+-mass: *m*/*z* (%) 1662.7 ([M^+], 100). The purity of **21** was established from clean multinuclear NMR spectra (see the Supporting Information in ref 4a).

{Cp*Co(2,3-$Et_2C_2B_4H_3$-7-C≡C)}$_3C_6H_3$ (22). Method A. To a solution of **4** (348 mg, 1 mmol) in 25 mL of THF was added *t*-BuLi (0.63 mL of a 1.6 M solution in hexane, 1 mmol) at 0 °C. After the solution was stirred for 0.5 h at 0 °C, anhydrous $ZnCl_2$ (136 mg, 1 mmol) in 8 mL of THF was added at 0 °C. The mixture was stirred at room temperature for 2 h, $C_6H_3I_3$ (137 mg, 0.3 mmol) and $Pd(PPh_3)_4$ (52 mg, 0.045 mmol) were added, and refluxing was continued for 16 h, after which the solvent was removed in vacuo. The residue was taken up in CH_2Cl_2 and flash-chromatographed through 3 cm of silica gel in CH_2Cl_2. Column chromatography of the CH_2Cl_2 wash in 1:1 hexane/CH_2Cl_2 yielded **22** as a major orange-yellow band (280 mg, 81.5%).

Method B. To a mixture of **4** (35 mg, 0.1 mmol), $Pd(PPh_3)_2Cl_2$ (3.5 mg, 0.005 mmol), CuI (2 mg, 0.01 mmol), and $C_6H_3I_3$ (13 mg, 0.03 mmol) were added 5 mL of THF and 1 mL of Et_3N. The mixture was stirred for 2 days, the solvent was removed in vacuo, and the residue was taken up in CH_2Cl_2 and flash-chromatographed through 3 cm of silica gel in CH_2Cl_2. TLC chromatography of the CH_2Cl_2 wash in 1:3 hexane/CH_2Cl_2 gave **22** as a major orange-yellow band (22 mg, 66%). ^1H NMR ($CDCl_3$): δ 1.31 (t, 18H, $J = 7.5$ Hz, ethyl CH_3), 1.77 (s, 45H, C_5Me_5), 2.26, 2.44 (sextet, 6H, $J = 7.5$ Hz, ethyl CH_2), 6.861 (s, 3H, C_6H_4). $^{13}C\{^1H\}$ NMR ($CDCl_3$): δ 10.0 (C_5Me_5), 14.5 (ethyl CH_3), 21.9 (ethyl CH_2), 86.6 (C≡C), 93.6 (C≡C), 91.0 (C_5Me_5), 92.1 (C_2B_4), 123.5 (C_6H_4), 133.8 (C_6H_4). ^{11}B NMR (75 °C, toluene-d_8): δ −2.3 (s, 3B), 3.9 (unresolved, BH, 6B), 7.9 (unresolved, BH, 3B). IR (KBr pellet, cm^{-1}): ν 2964.4 (s), 2931.9 (m), 2910.9 (m), 2873.9 (w), 2533.2 (vs, B−H), 2176.9 (w, C≡C), 1717.4 (m), 1715.3 (m), 1576.3 (s), 1476.3 (s), 1383.7 (s), 1219.3 (s), 1027.1 (m), 880.9 (m), 784.2 (vs). CI^+-mass: *m*/*z* (%) 1115.8 ([M^+], 100). UV−vis (CH_2Cl_2, nm (%)): 307 (100), 247 (23) ϵ_{max} 285 961 $cm^{-1}\ M^{-1}$. Anal. Calcd for $C_{60}H_{87}B_{12}Co_3$: C, 64.64; H, 7.87. Found: C, 64.74; H, 7.83.

{Cp*Co[2,3-$Et_2C_2B_4H_3$-7-$C_2Co_2(CO)_6$]}$_3C_6H_3$ (23). To a solution of $Co_2(CO)_8$ (34 mg, 0.1 mmol) in 4 mL of CH_2Cl_2 was slowly added **22** (33.5 mg, 0.03 mmol) in 6 mL of CH_2Cl_2 at 0 °C. After the solution was stirred for 3 days at room temperature, the solvent was removed and the residue was separated on TLC plates in 2:1 CH_2Cl_2/hexane to afford the red-brown solid **23** (33 mg, 55.7%). ^1H NMR ($CDCl_3$): δ 1.20 (t, 18H, $J = 7.5$ Hz, ethyl CH_3), 1.77 (s, 45H, C_5Me_5), 2.01, 2.30 (sextet, 6H, $J = 7.8$ Hz, ethyl CH_2), 7.040 (s, 3H, C_6H_4). ^{13}C NMR ($CDCl_3$): δ 10.1 (C_5Me_5), 14.3 (ethyl CH_3), 21.8 (ethyl CH_2), 90.8 (C_5Me_5), 100.0 (C−Co−C), 95.0 (C_2B_4), 129.0 (C_6H_4), 139.4 (C_6H_4), 199.5 (C−O). IR (KBr pellet, cm^{-1}): ν 2972.6 (m), 2934.3 (m), 2909.6 (m), 2542.2 (m, B−H), 2083.2 (vs, C−C), 2053.1 (vs, C−O), 2016.7 (C−O), 1560.2 (m), 11452.3 (m), 1383.3 (s), 1029.2 (m), 788.2 (m), 563.2 (m), 520.6 (s), 466.0 (s). UV−vis (CH_2Cl_2, nm (%)): 216 (100), 314 (21) $\epsilon_{max} = 108\ 836\ cm^{-1}\ M^{-1}$. Anal. Calcd for $C_{78}H_{87}B_{12}Co_9O_{18}$: C, 47.49; H, 4.45. Found: C, 47.67; H, 4.55.

X-ray Structure Determinations on 8 and 19. All diffraction data were collected on a Bruker SMART APEX CCD diffractometer at −120 °C using graphite-monochromated Mo Kα radiation ($\lambda = 0.710\ 73$ Å). A total of 1800 frames were collected for each crystal using ω scans. Empirical absorption corrections were applied using the Bruker SADABS program,[26] with the transmission factors ranging 0.59−0.80 and 0.73−0.80 for **8** and **19**, respectively. The structures were solved by direct methods within the Bruker SHELXTL program suite.[27] Full-matrix least-squares refinement on $|F|^2$ yielded the final R1 and wR2 values of 0.0516 and 0.1651 for **9** as well as 0.0598 and 0.1296 for **18**. Hydrogen atoms were placed in calculated positions, except those attached to the boron atoms, which were found in difference maps and refined with isotropic displacement parameters. The final difference Fourier maps were essentially featureless. Crystallographic data for both new structures in this paper have been deposited with the Cambridge Crystallographic Data Centre, CCDC Nos. 204135 (**8**) and 204136 (**19**). Copies of this information may be obtained free of charge from The Director, CCDC, 12 Union Road, Cambridge CB2 1EZ, U.K. (fax, +44-1223-336033; e-mail, deposit@ccdc.cam.ac.uk; web, http://www.ccdc.cam.ac.uk).

Electrochemistry. Anhydrous 99.9% HPLC grade dichloromethane for electrochemistry was purchased from Aldrich. Anhydrous 99.9% HPLC grade tetrahydrofuran for electrochemistry (purchased from Aldrich) was distilled over sodium before use. The supporting electrolyte used was either electrochemical grade $[NBu_4][PF_6]$, obtained from Fluka, or $[NBu_4][B(C_6F_5)_4]$, prepared as described in ref 10. Cyclic voltammetry was performed in a three-electrode cell having a platinum working electrode surrounded by a platinum-spiral counter electrode and an aqueous saturated calomel reference electrode (SCE) mounted with a Luggin capillary. Either a BAS 100A or a BAS 100W electrochemical analyzer was used as a polarizing unit. Controlled-potential coulometry was conducted in an H-shaped cell with anodic and cathodic compartments separated by a sintered-glass disk. The working macroelectrode was platinum gauze; a mercury pool was used as the counter electrode. All reported potential values are referred to the saturated calomel electrode (SCE).

Acknowledgment. Support from the National Science Foundation for the synthetic studies (Grant No. CHE-9980708 to R.N.G.) and for the purchase of a departmental CCD X-ray diffractometer (Grant No. CHE-9974875 to the Department of Chemistry) is gratefully acknowledged. P.Z. gratefully acknowledges the financial support of the University of Siena (PAR 2001).

Supporting Information Available: Tables of atomic coordinates, bond distances, bond angles, anisotropic thermal parameters, and calculated mean planes for **8** and **19**. This material is available free of charge via the Internet at http://pubs.acs.org.

OM0301379

---

(26) Sheldrick, G. M. SADABS: Program for Empirical Absorption of Area Detector Data; University of Gottingen, Gottingen, Germany, 1996.

(27) Sheldrick, G. M. *SHELXTL Version 5.1 Reference Manual*; Bruker AXS: Madison, WI, 1997.